

**Application Performance Evaluation for IBeacon
In-Room Localization Technology
Using CRLB**

By

Yang Yang

A Thesis

Submitted to the Faculty

of the

WORCESTER POLYTECHNIC INSTITUTE In

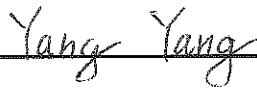
partial fulfillment of the requirements for the

Degree of Master of Science

In

Electrical and Computer

Engineering by



April 2016

APPROVED:



Professor Kaveh Pahlavan, Major Thesis Advisor



Professor Yehia Massoud, Head of Department

Abstract

This thesis is a part of a research project performed by two MS students, Zhouchi Li and the author. The overall objective of the project is the design, implementation and performance evaluation of algorithms for newborns localization and tracking in hospitals using Apple iBeacon technology. Although we were working on the project together, I lead performance evaluation of the in-room localization system using Cramer Rao Lower Bound (CRLB). My partner, Zhouchi Li, leads modeling the path-loss of iBeacons and presence detection algorithms. This thesis describes the project with a focus on my individual contributions in CRLB analysis under different iBeacon deployment patterns as well as performance evaluation using practical characteristics of shadow fading.

Today, Wi-Fi localization is the most popular indoor localization technique, which provides an accuracy of a few meters to distinguish the presences in different rooms of a building. With the recent introduction of iBeacon by Apple, possibility of more accurate in-room localization has emerged for specific applications such as locating newborns inside a hospital. The iBeacon uses Bluetooth Low Energy (BLE) technology that broadcasts beacons with unique information to the nearby receivable devices such as iPhone and android smart phones. The RSS of these beacons can be used to estimate the location and to construct an in-room localization system.

In this thesis, we investigate in-room localization system using iBeacon for the newborns in hospitals with an accuracy of about 1 meter. We firstly present an in-room localization system using RSS from iBeacon. Then, based on the traditional Cramer-Rao Lower Bound (CRLB) we analyze the optimal deployment strategy for different iBeacon deployment patterns in the nursery room. Finally, we introduce a novel approach for calculation of the CRLB which includes practical conditions to analyze the influence of variable variance of shadow fading and coverage probability.

**Application Performance Evaluation for iBeacon
In-Room Localization Technology
Using CRLB**

By

Yang Yang

A Thesis

Submitted to the Faculty

of the

WORCESTER POLYTECHNIC INSTITUTE In

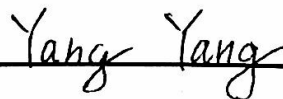
partial fulfillment of the requirements for the

Degree of Master of Science

In

Electrical and Computer

Engineering by



April 2016

APPROVED:


Professor Kaveh Pahlavan, Major Thesis Advisor


Professor Yehia Massoud, Head of Department

Acknowledgements

I would like to express my gratitude to my advisor Professor Kaveh Pahlavan who made sure the thesis has 99 pages, 41 pictures and lots of formulas and thus made my master thesis much more native and well organized.

My thanks are also due to my partner Zhouchi Li, who has worked with me in this project for more than 1 year that without him I will never be able to complete this thesis.

Thanks also to my dear friend Julang Ying, who helped me a lot in the CRLB analysis part that his math ability makes me better understand the meaning of CRLB and thus comes a main part of my thesis.

More thanks to lots of friends, whenever I face a problem, there are always friends around me that not only help me in solving the problem, but also keep my heart warm which supports me to continue my research all the time.

That is all, great thanks to all my dears.

Contents

Abstract	2
Acknowledgements.....	3
Contents	4
List of Figures	7
List of Table	10
Chapter 1 Introduction.....	1
1.1 Project background and motivation	1
1.2 Contributions of this thesis	2
1.3 Thesis outlines	3
Chapter 2 Backgrounds in in-room localizations.....	4
2.1 iBeacon and BLE communication	4
2.2 Fading margin and shadow fading	11
2.3 In-room presence detection	15
2.4 In-room localization in hospitals.....	16
2.5 Cramer–Rao bound	20
Chapter 3 Algorithms for intelligent in-room presence detection using iBeacon	22
3.1 Ibeacon application development.....	22

3.1.1	Development using objective C	24
3.1.2	Self-developed application	26
3.2	Two approaches of presence detection.....	27
3.2.1	Double iBeacons approach.....	29
3.2.2	Single iBeacon approach.....	31
3.2.3	Comparison	32
Chapter 4	Methodology and discussion for in-room Localization using iBeacon.....	34
4.1	Path-loss modeling.....	34
4.1.1	RSSI data collection system.....	34
4.1.2	Modeling and validation.....	35
4.1.3	Discussion of path-loss modeling	38
4.2	Scenarios and algorithms of in-room Localization.....	39
4.3	Methodology for performance evaluation.....	40
4.3.1	Scenarios for performance evaluation.....	41
4.3.2	Localization error estimation of deployment patterns.....	42
4.3.3	CRLB for performance evaluation in 3D.....	44
4.4	Effect analysis of different deployment methods.....	46
4.4.1	Effect of different deployment patterns.	46
4.4.2	Effect of different number of iBeacons.....	48

Chapter 5	Performance evaluation for in-room localization technology using iBeacon	51
5.1	Coverage possibility	52
5.2	CRLB with coverage probability and variable shadow fading	56
5.3	Discussions in CRLB with coverage probability and variable shadow fading	61
5.3.1	Comparison with traditional CRLB	61
5.3.2	Relationship between iBeacon coverage and room size	64
Chapter 6	Conclusions and future works	68
Bibliography		70
Appendix		78
A.	Matlab code for path-loss modeling and Cramer-Rao lower bound calculation:	78
B.	Matlab code for Cramer-Rao lower bound considering coverage probability and variable shadow fading:	82

List of Figures

Figure 2.1 Menu of Estimote iBeacon application 1.....	6
Figure 2.2 Menu of Estimote iBeacon application 2.....	7
Figure 2.3 Menu of Estimote iBeacon application 3.....	8
Figure 2.4 Frame of iBeacon communication 1.....	9
Figure 2.5 Frame of iBeacon communication 2.....	10
Figure 2.6 Relationship between variable shadow fading and distance	12
Figure 3.1 Frame of iBeacon application development	23
Figure 3.2 Menu of self-developed iBeacon application.....	24
Figure 3.3 Menu of coding in Objective-C	25
Figure 3.4 Menu of receiving data in server	26
Figure 3.5 Menu of server by using Python	27
Figure 3.6 Algorithm for presence detection using 2 iBeacons.....	28
Figure 3.7 Algorithm for presence detection using 1 iBeacon.....	29
Figure 3.8 RSSI plot for double iBeacon approach, for the MH entering movement	30
Figure 3.9 RSSI plot for double iBeacon approach, for the MH opening the door without entering/leaving	30

Figure 3.10 RSSI plot for single iBeacon approach, for the MH entering movement	32
Figure 3.11 RSSI plot for various iPhone positions	33
Figure 4.1 Two path-loss models comparison	36
Figure 4.2 Comparison of cumulative distribution functions of distance measurement error in two models	37
Figure 4.3 Scenario for in-room localization	39
Figure 4.4 Scenario of RSS ranging localization	40
Figure 4.5 Scenarios of different deployment methods	41
Figure 4.6 Contour of estimate location error in 2D in scenario 1.....	43
Figure 4.7 Contour of estimate location error in 2D in scenario 2.....	43
Figure 4.8 Contour of estimate location error in 2D in scenario 3.....	44
Figure 4.9 Contour of estimate location error in 3D	46
Figure 4.10 Comparison of cumulative distribution functions of CRLB in 3 different deployment patterns	47
Figure 4.11 Contour of estimate location error of 3 iBeacons	48
Figure 4.12 Contour of estimate location error of 4 iBeacons	49
Figure 4.13 Contour of estimate location error of 5 iBeacons	49
Figure 4.14 Comparison of cumulative distribution functions of CRLB in different number of iBeacons	50

Figure 5.1 Relationships between coverage possibility and distance	53
Figure 5.2 CRLB under practical conditions with different number of access points	59
Figure 5.3 CRLB under practical conditions with all 4 access points	60
Figure 5.4 Scenario of localization using 4 iBeacons	61
Figure 5.5 CRLB under practical conditions with 4 iBeacons	62
Figure 5.6 Traditional CRLB with 4 iBeacons	62
Figure 5.7 Comparison of cumulative distribution functions of traditional CRLB and CRLB under practical conditions	63
Figure 5.8 Mean of CRLB under practical conditions versus reliable coverage rate (reliable iBeacon coverage divided by room size).....	65
Figure 5.9 Standard variance of CRLB under practical conditions versus reliable coverage rate (reliable iBeacon coverage divided by room size).....	66
Figure 5.10 Comparison of cumulative distribution functions of CRLB under practical conditions in different reliable coverage rates	67

List of Table

Table 3.1 Performance of proposed in-room presence detection approaches	32
Table 4.1 Parameters of two different path-loss models	38
Table 4.2 Distance measurement error comparison of two models	38
Table 4.3 Comparison of CRLB in 3 different deployment patterns	47
Table 4.4 Comparison of CRLB in different number of iBeacon	50
Table 5.1 Mean and standard variance of cumulative distribution functions of traditional CRLB and CRLB under practical conditions	64

Chapter 1

Introduction

iBeacon is a class of Bluetooth Low Energy (BLE) devices introduced by Apple in 2013 that broadcast unique information to the nearby receivable devices. There are 3 parts in this unique information packet: Universally Unique Identifier (UUID), major, and minor which can all be defined by the users. Once these iBeacons are detected, the receivers are able to estimate the proximity according to the Received Signal Strength (RSS) of the iBeacon. In brief, iBeacon functions like the ancient beacon in the ocean except sending Bluetooth Low Energy signal rather than light to the receivers. Compared with traditional Bluetooth technology, BLE is intended to have similar coverage area while less power consumption. This makes it possible that iBeacon can be used for several years without changing battery. Furthermore, it is not necessary for such devices using BLE signal to pair with each other before they communicate. Nowadays almost all the smart phones, like iPhone, Android and Blackberry, are compatible with BLE technology which indicates that they can all collaborate with iBeacons. More importantly, there is no need for us to install special BLE receivers for iBeacon since almost everyone owes a smart phone. iBeacon has many location-based applications. One of the most outstanding aspects that attracts more and more industries' attention is to develop indoor positioning systems. Not only Apple but enterprises such as Qualcomm, PayPal, and SKT are looking forward to face another evolution by partnering with newest devices such as iBeacon.

1.1 Project background and motivation

There exist some differences between iBeacon and other traditional indoor localization technologies. First of all, the signal that iBeacon transmits is a one-way broadcast, which

means only the receiving devices can get information from iBeacon, but they cannot send back any information to iBeacon. Second, users are required to install an application on their receiving devices (smartphones) to receive BLE signal, which will help them to protect their privacy because only the applications rather than iBeacons may obtain their position information.

Even though outdoor localization is quite mature and has been implemented in our daily life such as the vehicle navigation with the advancement of localization technology, there are a huge amount of indoor smartphone applications which demonstrate an intense need to the position information of the users, so that plenty of position-based applications are achievable. However, traditional outdoor localization technologies cannot solve this problem successfully like GPS performs awful in indoor environment that is why we focus on in-room localization using iBeacon.

1.2 Contributions of this thesis

This thesis is a part of a research project performed by two MS students, Zhouchi Li and the author. The overall objective of the project is the design, implementation and performance evaluation of algorithms for newborns localization and tracking in hospitals using Apple iBeacon technology. During this project, we have already submitted two conference papers:

1. Yang Yang, Zhouchi Li and Kaveh Pahlavan, "Using iBeacon for intelligent in-room presence detection", 2016 IEEE CogSIMA, San Diego, CA, Mar. 2016.
2. Zhouchi Li, Yang Yang and Kaveh Pahlavan, "Using iBeacon for Newborns Localization in Hospitals", 2016 IEEE 10th ISMICT, Worcester, MA, Mar. 2016.

Although we were working on the project together, I lead performance evaluation of the in-

room localization system using Cramer Rao Lower Bound (CRLB). My partner, Zhouchi Li, leads modeling the path-loss of iBeacons and presence detection algorithms. This thesis describes the project with a focus on my individual contributions in two major aspects: Analyze the optimal deployment strategy for different iBeacon deployment patterns in the nursery room and introduce a novel approach for calculation of the CRLB which includes practical conditions to analyze the influence of variable variance of shadow fading and coverage probability.

1.3 Thesis outlines

In this thesis, we investigate in-room localization system using iBeacon with an accuracy of about 1 meter. In chapter 1, we give a brief introduction to the motivation, contributions and outlines of this thesis. In chapter 2, backgrounds about iBeacon and BLE communications, fading margin and shadow fading, in-room presence detection and localization as well as Cramer Rao bound are presented. In chapter 3, a self-developed application is demonstrated and 2 algorithms are constructed by my partner Zhouchi Li and me to build a presence detection system that can inform us the number of people in a room. Then we focus on in-room localization which is described in chapter 4 and 5 to find out the positions of each people, considered as the next stage of our project. In chapter 4, methodology and discussion for in-room localization using iBeacon are presented. After path-loss modeling we compare the cumulative distribution functions (CDF) of the error in different deployment patterns as well as different number of iBeacons to find out the best deployment method of iBeacons. In chapter 5, we analyze the Cramer-Rao Lower Bound (CRLB) of localization considering coverage probability and variable shadow fading to evaluate the performance of in-room localization using iBeacon. Not only detailed analyses but also simulation results are illustrated in order to support our claims. In chapter 6, we make conclusions of the whole thesis and demonstrate our future works.

Chapter 2

Backgrounds in in-room localizations

Accurate in-room positioning information makes it possible to revolutionize the way people search, locate and navigate to points of interest inside rooms that is similar to how GPS revolutionized the way people navigate outdoors [1][2]. For instance, a mobile holder (MH) in a mall could leverage his mobile device to instantly search, locate and navigate with real-time directions to any store in the mall based on amateur indoor localization technology. In in-room scenario, the MH could automatically receive directions to the exact section where the desired product locates. Meanwhile, businesses and advertisers could push coupons and offers to the MH based on his position simultaneously insider a store to maximize customer shopping effectiveness [2]. Enabling such scenario has been challenging mainly due to the unreliability of GPS localization in indoor or in-room environments [3][4]. Due to the absence of GPS, we basically utilize iBeacons to complete in-room localization by using RSS-based localization technology which is similar to Wi-Fi localization. In this chapter, we introduce some backgrounds about iBeacon and its BLE communication, fading margin, in-room presence detection, in-room localization and Cramer–Rao bound that are useful in better understanding this thesis.

2.1 iBeacon and BLE communication

Presence detection is a common application for smart phones, which may contribute to energy-efficient intelligent lighting control, smart heating and air-conditioning, home

security system and etc. In public area, the in-room presence detection technologies can be also used to count the registration and check-in of an event. Existing literature introduces two major technical trends to implement in-room presence detection systems. At the beginning stage, the research community mounts various sensors to the room ceiling and tries to cover the room as much as possible. Sujin et. al [5], proposed a digital camera and image processing based presence detection system using intensity average variation to detect moving objects; Neubiberg et. al [6], presents a 360o rotational camera based approach to enhance the camera coverage.

The above mentioned first technical trend suffers from certain disadvantages. First and foremost, the pre-deployment of the infrastructure is not unified. Take the Prema™ as an example, only single sensor is required to cover a squared room but multiple sensors are necessary for an irregularly shaped room. As a consequence, the infrastructure cost is site-specific and it can goes exponentially high. To address that issue, the second trend locates sensors only to the entrance of the room. Motion sensors and infrared sensors [7][8] are attached to the room entrance to count either entering or leaving of the individuals. Such techniques successfully cut down the cost but it still suffer the lack of ability to identify the presented individuals.

iBeacon based system in this work is a potentially good choice without all above imperfections. With highly limited cost and long enough battery life, iBeacon is able to perform proximity estimation and at the same time identify the adjacent individuals. It also carries various other additional functionalities such as smart advertising [9]. Considering the advantages of iBeacon, we propose to use iBeacon for presence detection in this work.

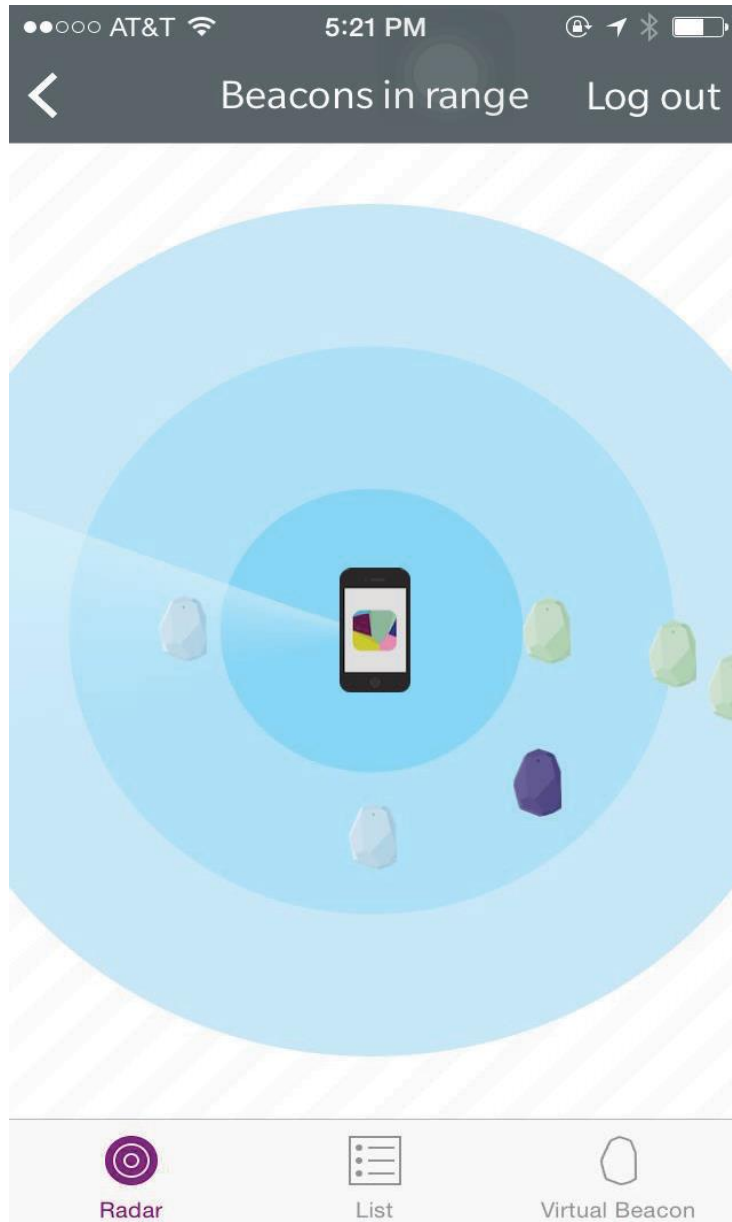


Figure 2.1 Menu of Estimote iBeacon application 1

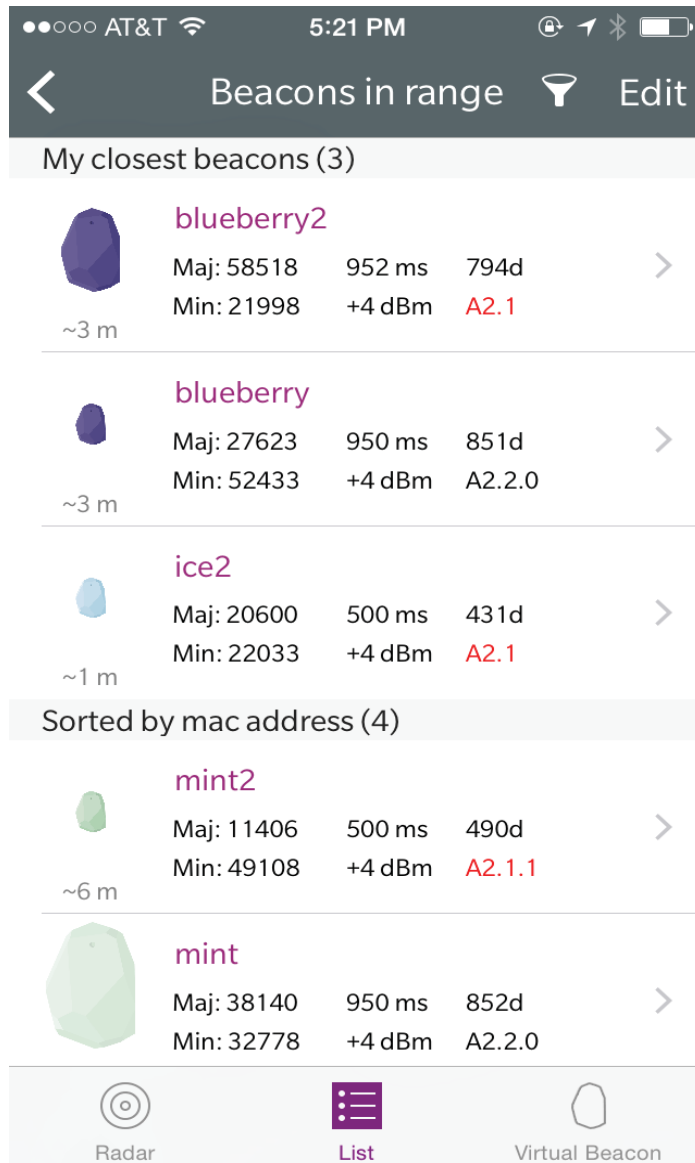


Figure 2.2 Menu of Estimote iBeacon application 2

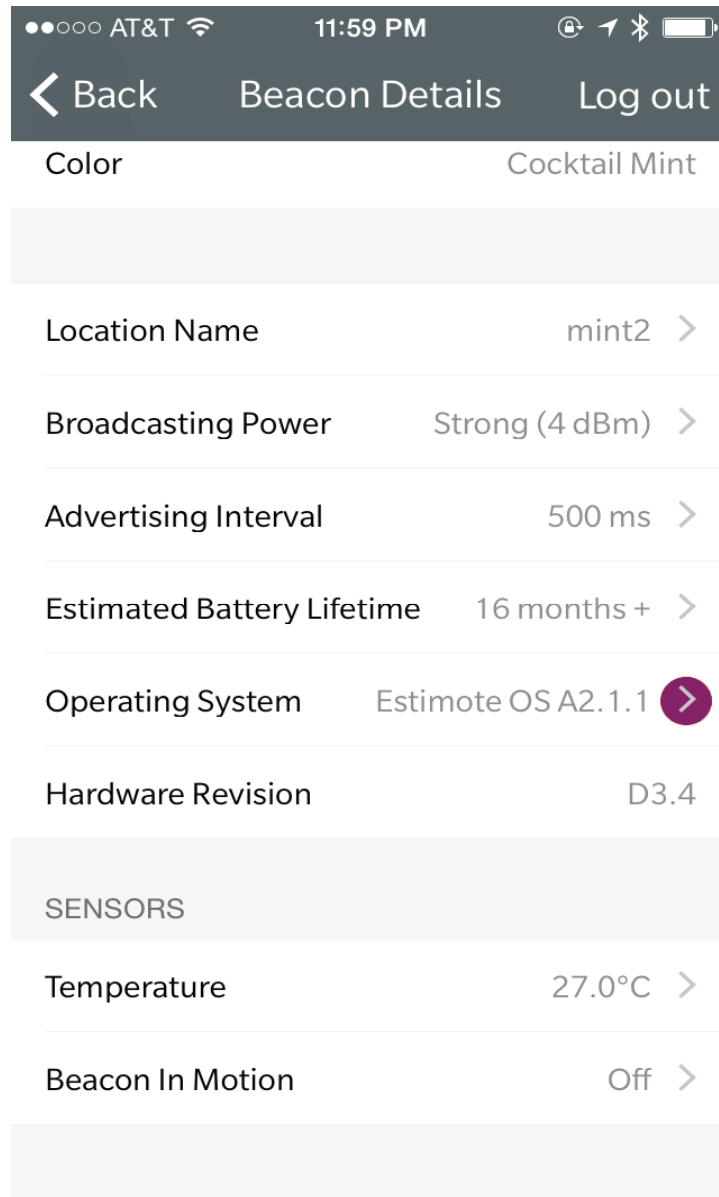


Figure 2.3 Menu of Estimote iBeacon application 3

The manufacturer of iBeacon, Estimote Company, provides their own iBeacon APP, which serves as a proximity estimator. The APP presents a graphic user interface (GUI) to display the geometric relationship between the iPhone and surrounding iBeacons. It also provides iBeacon ID, iBeacon status, distance between iBeacon and iPhone, iBeacon sensor reading and other information.

Typical screenshots of this Estimote APP has been depicted in Figure 2.1- Figure 2.3. It is very obvious that the Estimote APP has two major disadvantages considering the purpose of this paper. (1) Originally the APP is not designed to perform presence detection; (2) The APP fails to explicitly provide the RSSI reading. Given those disadvantages, it is necessary to design our own APP to achieve intelligent in-room presence detection.

BLE communication consists primarily of “Advertisements”, or small packets of data, broadcast at a regular interval by Beacons or other BLE enabled devices via radio waves [10]. BLE Advertising is a one-way communication method. Beacons that want to be “discovered” can broadcast, or “Advertise” self-contained packets of data in set intervals. These packets are meant to be collected by devices like smartphones, where they can be used for a variety of smartphone applications to trigger things like push messages, app actions, and prompts. This overall frame can be viewed in Figure 2. 4 and Figure 2. 5.

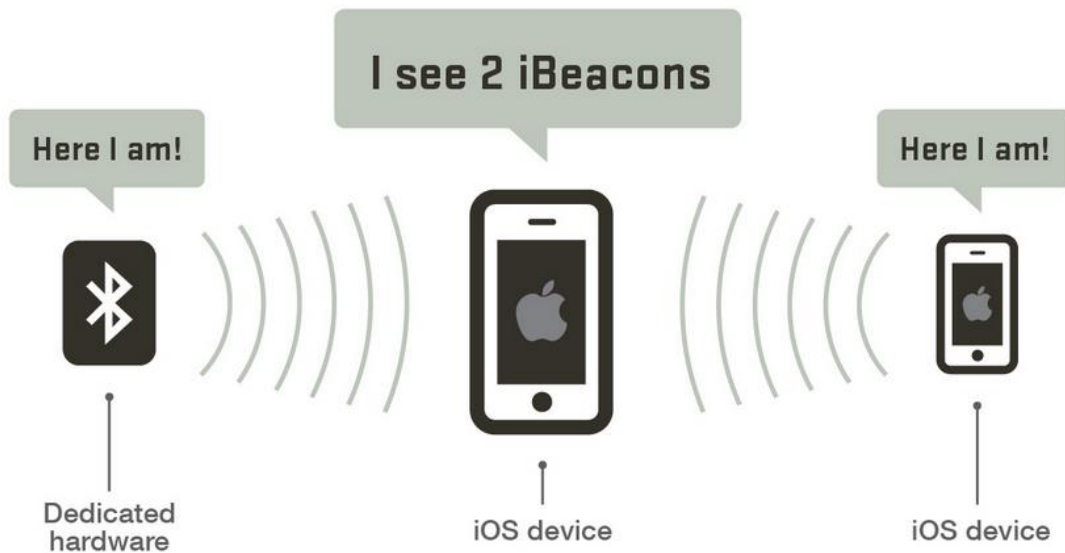


Figure 2.4 Frame of iBeacon communication 1

Apple’s iBeacon standard calls for an optimal broadcast interval of 100 ms. Broadcasting more frequently uses more battery life but allows for quicker discovery by smartphones

and other listening devices. Standard BLE has a broadcast range of up to 100 meters, which make Beacons ideal for indoor location tracking and awareness.

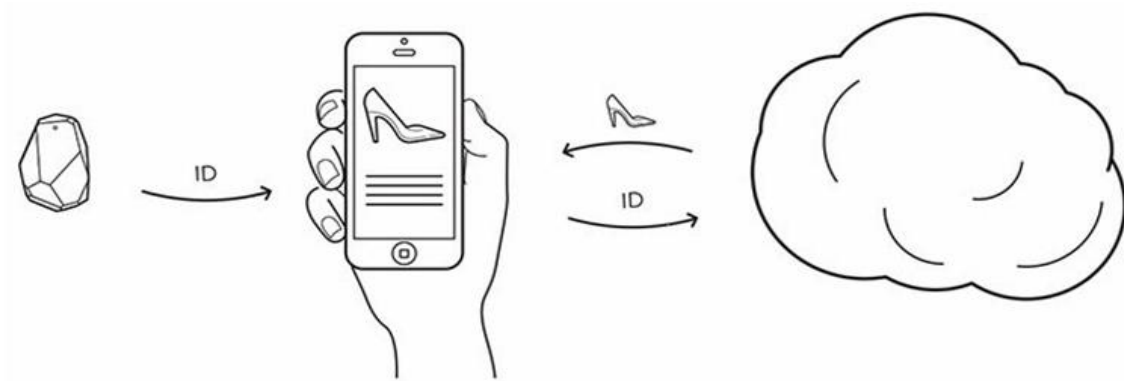


Figure 2.5 Frame of iBeacon communication 2

With iBeacon, Apple has standardized the format for BLE Advertising. Under this format, an advertising packet consists of four main pieces of information [10]:

UUID: This is a 16 byte string used to differentiate a large group of related beacons. For example, if Coca-Cola maintained a network of beacons in a chain of grocery stores, all iBeacons would share the same UUID. This allows Coca-Cola's dedicated smartphone app to know which beacon advertisements come from Coca-Cola-owned beacons.

Major: This is a 2 byte string used to distinguish a smaller subset of beacons within the larger group. For example, if Coca-Cola had four beacons in a particular grocery store, all four would have the same Major. This allows Coca-Cola to know exactly which store its customer is in.

Minor: This is a 2 byte string meant to identify individual beacons. Keeping with the Coca-Cola example, a beacon at the front of the store would have its own unique Minor. This allows Coca-Cola's dedicated app to know exactly where the customer is in the store.

Tx Power: This is used to determine proximity (distance) from the beacon. TX power is defined as the strength of the signal exactly 1 meter from the device. This has to be calibrated and hardcoded in advance. Devices can then use this as a baseline to give a rough distance estimate.

2.2 Fading margin and shadow fading

In reality at a distance d we have a 50% probability of having adequate signal strength (RSS that is larger than the receiver sensitivity). This is because the normally distributed (in dB) shadow fading random variable can have a positive value with 50% probability and that positive value increases the path loss beyond what was used for calculation of the distance d . For a terminal located in distance d from the base station, we have a 50% probability to operate with the required minimum signal strength. To increase this probability one may add power to increase the probability of coverage at distance d . This additional power is referred to as fading margin, and it is represented by $F\sigma$ [11].

We know that deviations of the average RSS from the best-fit line is caused by the changes in the pattern of obstructions shadowing the direct transmission and for that reason it is referred to as shadow fading. Shadow fading not only causes variations in the average RSS at the same distance, as we move away from the transmitter along a straight line, the power deviates randomly from the power predicted by the best fit line [12]. Therefore, shadow fading causes fluctuations in the average RSS when the distance is kept fixed and deviations from the best linear fit to the RSS as we move away from the transmitter.

In the former chapters of this thesis, all the shadow fading values, or the standard

variances of shadow fading, are considered as constants, typically we use 5 dB or 8 dB. However, [13] shows the fact that the shadow fading values are related with the distance. In his thesis, he introduced a statistical RF signal shadow fading model based on the measurements in a typical office building. This model related the shadow fading to the distance and uses two different distribution functions to approximate the shadow fading between the breaking point. Since the ranging based RSS localization algorithm and the fingerprint localization algorithm are widely used these days, we use this distance related shadow fading model to the further analysis of its effect on these localization algorithms. Based on their research, we can see the relationship in Figure 2.6:

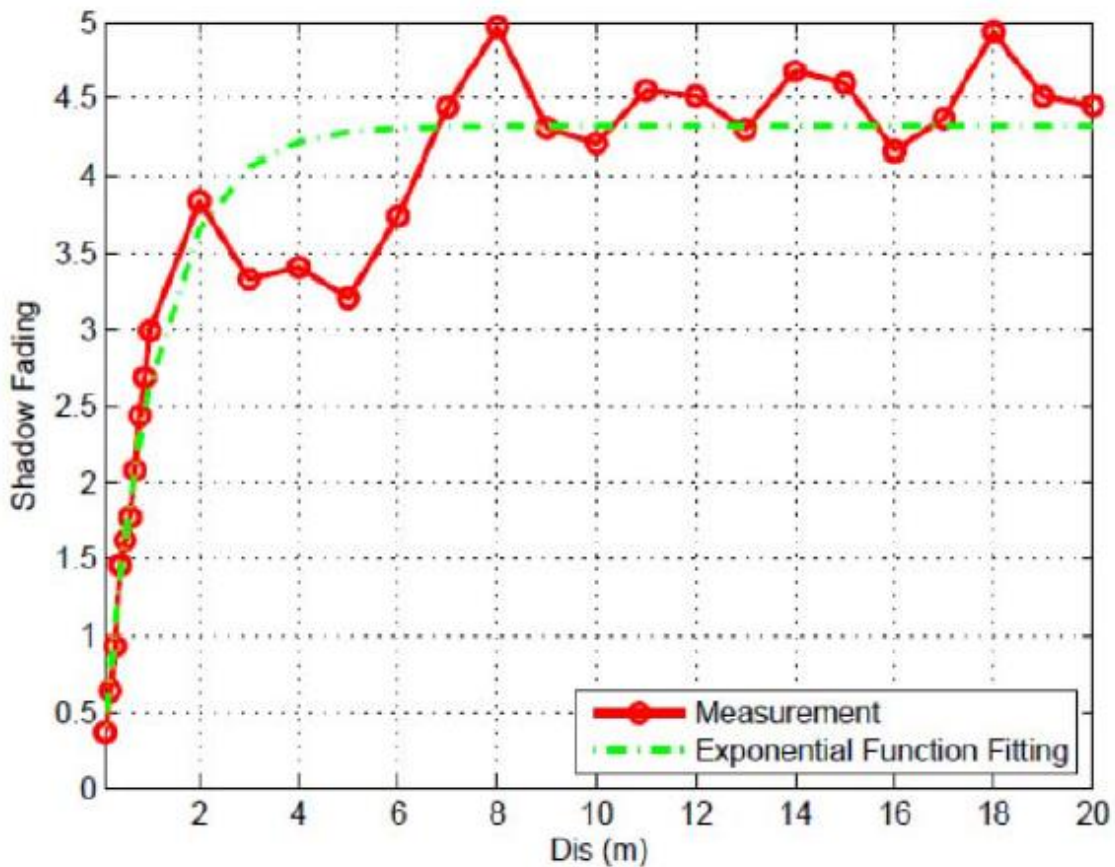


Figure 2.6 Relationship between variable shadow fading and distance

This relationship can be fitted by this equation [13]:

$$\sigma = -4.28 \times e^{-0.9372 \times d} + 4.31$$

In reality, the shadow fading, which is used to reflect the complexity of the environment, should be sensitive to the slight changes of the physical environment during the experiment. Therefore, the shadow fading should be fluctuated when the distance between the transmitter and receiver is changed. It is also what we use in the calculation of revised CRLB in the section 5.2.

In wireless communications, fading is deviation of the attenuation affecting a signal over certain propagation media. The fading may vary with time, geographical position or radio frequency, and is often modeled as a random process. A fading channel is a communication channel that experiences fading [11]. In wireless systems, fading may either be due to multipath propagation, referred to as multipath induced fading, or due to shadowing from obstacles affecting the wave propagation, sometimes referred to as shadow fading.

Shadowing is the effect that the received signal power fluctuates due to objects obstructing the propagation path between transmitter and receiver. These fluctuations are experienced on local-mean powers, that is, short-term averages to remove fluctuations due to multipath fading.

Experiments reported by Egli in 1957 showed that, for paths longer than a few hundred meters, the received (local-mean) power fluctuates with a 'log-normal' distribution about the area-mean power. By 'log-normal' is meant that the local-mean power expressed in logarithmic values, such as dB or neper, has a normal (i.e., Gaussian) distribution.

Egli studied the error in a propagation model predicting the path loss, using only distance, antenna heights and frequency. For average terrain, he reported a logarithmic standard deviation of about $s = 8.3$ dB and 12 dB for VHF and UHF frequencies, respectively. Such large fluctuations are caused not only by local shadow attenuation by obstacles in the vicinity of the antenna, but also by large-scale effects (hills, foliage, etc.) along the path profile, which cause attenuation. Hence, any estimate of the area-mean power which ignores these effects may be coarse.

This log-normal fluctuation was called 'large-area shadowing' by Marsan, Hess and Gilbert. They measured semi-circular routes in Chicago, thus fixing distance to the base station, antenna heights and frequency, but measuring different path profiles. The standard deviation of the path loss ranged from 6.5 dB to 10.5 dB, with a median of 9.3 dB. This 'large-area' shadowing thus reflects shadow fluctuations if the vehicle moves over many kilometers.

In contrast to this, in most papers on mobile propagation, only 'small-area shadowing' is considered: log-normal fluctuations of the local-mean power are measured when the antenna moves over a distance of tens or hundreds of meters. Marsan et al. reported a median of 3.7 dB for small area shadowing. Preller and Koch measured local-mean powers at 10 m intervals and studied shadowing over 500 m intervals. The maximum standard deviation experienced was about 7 dB, but 50% of all experiments showed shadowing of less than 4 dB.

In a radio system, an allowance made so that a signal can fade up to a given amount, while still maintaining overall performance at an acceptable level. For example, an RF signal may be attenuated by a given number of decibels, yet sustain a signal-to-noise ratio

above a specified minimum. Also it is called fading margin which is a designed allowance that provides for sufficient system gain or sensitivity to accommodate expected fading, for the purpose of ensuring that the required quality of service is maintained. The amount by which a received signal level may be reduced without causing system performance to fall below a specified threshold value. It is mainly used to describe a communication system such as satellite, for example a system like global star operates at 25-35 dB Fade margin. This fading margin in RSS based localization gives us a suggestion about what is the reliability of locate result in such distance, based on which we can calculate the detection possibility by access points or iBeacons.

2.3 In-room presence detection

iBeacon has many location-based applications. It can be used to develop indoor positioning systems [14][15]. It can be used to build an indoor proximity estimation system to detect the number of moving objects in a room, and even gather the patterns of their movement [16]. Moreover, iBeacons can be also used as launching APPs on remote devices [17]. The interest of industry for iBeacon is increasing as well. Not only Apple but enterprises such as Qualcomm, PayPal, and SKT carry forward related businesses by partnering with a variety of companies [18].

The hardware basis of this work is the iBeacon transmitters from Estimote [19], cooperating with the most recent iPhone 5s, 6/6Plus and 6s/6sPlus. We develop our intelligent in-room presence detection system using existing APIs which provide received signal strength indicator (RSSI) and the motion information. Most importantly, we managed to manipulate empirical data and decide whether a person is in-room or not.

In this thesis, we assume that the entrance door automatically shuts after an individual

goes into or out of the room. When the individual opens and gets through the door with our APP properly launched, our APP receives the beacon signal and sends the beacon RSSI to the server. The server archives the RSSI and decides the presence status of that individual according to computational result of our algorithm. We first and foremost focus on the system implementation with two iBeacons, one of them attached to the outside of door while another mirroring at the inside. Such implementation provides adequate understanding on the physical phenomenon. After that, we move on to single iBeacon implementation, for which our system still performs well enough, but works with less expenses and more convenience.

2.4 In-room localization in hospitals

In hospitals one of the most important tasks is the safety of patients and indoor positioning service can help improve patient safety. Among numerous in-room positioning technologies, Wi-Fi localization is widely used in the hospital today [20]. This is for indoor geolocation in an entire building assuming that the user uses a smart phone. With the help of these kinds of position-based applications, doctors and nurses will master the health conditions of patients easily and timely. Another application is finding newborn babies in the nursery rooms. In the application they put a tag at the babies' legs or wrists and use RFID to identify and track babies [21].



Fig.1 Radio Frequency Identifier tag used in nursery room

In this thesis we use iBeacon, a Bluetooth Low Energy (BLE) based technology, to replace RFID for in-room localization in this paper. Compared with expensive special-purpose RFID reader infrastructure (such as commercial UHF RFID readers or USRPs), the cost of the iBeacon deployment is much lower because BLE capable devices are already nearly ubiquitous as essentially all smart phones, tablets, and PCs from major manufacturers such as Apple and Samsung have adopted the Bluetooth 4.0 standard, which includes BLE as a key mode of operation [22]. The working coverage of iBeacon is also larger than that of RFID, but smaller than WiFi. If the working range is a whole building, not a single room, WiFi localization may be a better choice. The hardware basis

of this work is the iBeacon transmitters from Estimote [10], cooperating with the most recent iPhone 5s, 6/6Plus and 6s/6sPlus.

By putting an iBeacon on every baby's leg and use the iBeacon to broadcast the unique ID information, we can identify babies on users' smart phone [23]. Furthermore, if we predefine a distribution map of all the iBeacons in the nursery room, we can locate the users and navigate them to a certain baby according to RSSI analysis. Different deployment patterns will result in different localization performance, which can be quantified by our path-loss modeling and 3D CRLB analysis of iBeacons [24].

With the development of WLANs (Wireless Local Area Networks), there is an increasing level of interest in developing the technology to "geolocate" users in an indoor environment. Positioning and tracking of an indoor user based on radio signals will encounter a considerable degree of technical difficulty because various objects such as floors, walls and human bodies within a confined space will contribute to a rather complex form of attenuation and fading of the radio signals to be used for geolocation. [25] A majority of wireless geolocation techniques are based on such information as TOA (the time of arrival), TDOA (the time difference of arrival), and DOA (the direction of arrival). But geolocation based on these techniques is reliable only when line-of-sight signals are dominant, hence it will not be applicable to an indoor environment. Furthermore, a TOA or TDOA based approach requires accurate synchronization between transmitters and receivers.

We therefore explore an alternative geolocation method, that is, a signal strength based approach. Instead of measuring the time or angle of signal arrival, the signal strength method makes use of the level of signal power (or energy) sensed by an MS (mobile station) regarding the signals transmitted by reference base stations or APs (access points

in the IEEE802.11 terminology). This signal strength based approach may be also possible in a reversed situation, where the signal from an MS is sensed by multiple APs. This second approach would relieve an individual MS from the task of computing its position or processing and transferring relevant information to some BS (base station) or AP, as would be required in the first approach. However, a set of signals from different MSs must be designed in such a manner that APs can distinguish the signals from different MSs.

As early as in the 1960's, the signal attenuation model has been proposed as an approach to locate vehicles in motion on the street. [25] Nevertheless, the signal strength based geolocation is still an unexplored technique for locating WLAN users in an indoor environment. In our research we use, as our starting point, a recent work reported by Bahl and Padmanabhan. [25] Before reviewing their analysis, we first introduce a simple signal propagation model which is based on a signal predictor variable, where the observed variable is the signal strength (in dBm), and the predictor (or controlled) variable is the distance from a reference position (also in logarithm), and the main parameter to be estimated (i.e., regression coefficient) is the exponent value α that determines path loss of the signal when the distance from the signal source is given. Then we use Bahl's empirical signal propagation model which is also based on a linear regression analysis and in which the observed variable of signal strength has been compensated for the attenuation caused by the walls intervening between the MS and AP before applied to the regression analysis. We then extend this linear regression model to a multiple regression model by adding another predictor variable, i.e., the wall attenuation factor, denoted WAF [dB]. There may exist walls intervening between a possible MS location (to be estimated in geolocation) and a given reference position. We then evaluate

the improvement of this multiple regression model over the linear regression model by comparing their coefficients of determination and standard deviations. In order to carry out this statistical analysis, we resort to a simulation technique.

2.5 Cramer–Rao bound

In estimation theory and statistics, the Cramer–Rao bound (CRB) or Cramer–Rao lower bound (CRLB), named in honor of Harald Cramer and Callyampudi Radhakrishna Rao who were among the first to derive it, they express a lower bound on the variance of estimators of a deterministic parameter. The bound is also known as the Cramer–Rao inequality or the information inequality.

In its simplest form, the bound states that the variance of any unbiased estimator is at least as high as the inverse of the Fisher information. An unbiased estimator which achieves this lower bound is said to be (fully) efficient. Such a solution achieves the lowest possible mean squared error among all unbiased methods, and is therefore the minimum variance unbiased (MVU) estimator. However, in some cases, no unbiased technique exists which achieves the bound. This may occur even when an MVU estimator exists.

The Cramer–Rao bound can also be used to bound the variance of biased estimators of given bias. In some cases, a biased approach can result in both a variance and a mean squared error that are below the unbiased Cramer–Rao lower bound [26].

There is a wide range of wireless sensor network (WSN) applications requiring knowledge of sensor locations, from indoor user tracking to environmental and structural monitoring. Location estimation schemes used in long-range communications, such as

wireless cellular networks (WCN), include time of arrival (TOA), time difference of arrival (TDOA), and received signal strength (RSS). Although RSS measurements are easily available, since mobile terminals (MT) constantly monitor the strength of the neighboring base stations' pilot signals for handoff purposes [27], the RSS technique has been circumvented in WCNs, because of its dependency on the distance of the located device to the reference devices (i.e. base stations). In WSNs, on the other hand, the distances between mobile sensor nodes (SN) and the neighboring reference devices are by an order of magnitude smaller than in WCNs. For example, in the emerging ZigBee standards, the transmission range of reduced function devices (RFD) and full function devices (FFD) are set to be 30 meters. At this range, RSS-based location estimation performs better.

Chapter 3

Algorithms for intelligent in-room presence detection using iBeacon

This chapter focuses on how to establish an intelligent in-room presence detection system using iBeacon. With the help of this system, the attendance registration of large rallies like courses and seminars can be completed automatically and the system can be used for any meeting places without frequent charging. Moreover, the system can also be integrated into indoor localization systems, which will lead us to more applications. In order to construct this presence detection system step by step, we firstly analyze the differences between existing marketable iBeacon APPs and our own APP. With the explanation of the experimental setup for both two iBeacons and one iBeacon scenarios, we present the details of our presence detection algorithms and systems, and then we focus on system performance and validation. Finally, we draw our conclusions and make discussions.

3.1 iBeacon application development

The iBeacons produced by Estimote Company can provide us much information we need such as RSS, broadcasting interval, minor and major values and even motion sensor [19]. However, the existing app from Estimote Company do not allow us to collect data directly from iPhone which means large samples are impossible and we can only collect data by hand. Even though the application provided by Estimote Company can satisfy many requirements in iBeacon, there is an unavoidable problem existing in this application: we cannot extract any data from this application which means the RSS data

we need can only be recorded by hand that is absolutely inconvenient and impossible for large data. To solve this problem, we decide to develop our own app. Since intuitively we know that the geometric relationship between the iBeacon and iPhone can be reflected by the RSSI fluctuation of beacon signal, we employ necessary APIs to get the RSSI reading directly from iPhone sensors. The APP encapsulates three essential information into each record, including the iBeacon ID, RSSI reading and Time stamp. Considering the scalability of the system, iBeacon ID has been partitioned into Universally Unique Identifier (UUID), Major field, and Minor field [28]. In that sense, for large scale deployment, we may configure building number as iBeacon UUID, floor number as iBeacon Major and the iBeacon indicator as iBeacon Minor. The structure of each record can be given as

{UUID, Major, Minor, RSSI, Time stamp}

Typical screenshot of our own APP has been depicted in Figure 3.2, in which we explicitly display Major, Minor and RSSI fields but implicitly record the UUID and Time stamp for privacy concerns.



Figure 3.1 Frame of iBeacon application development

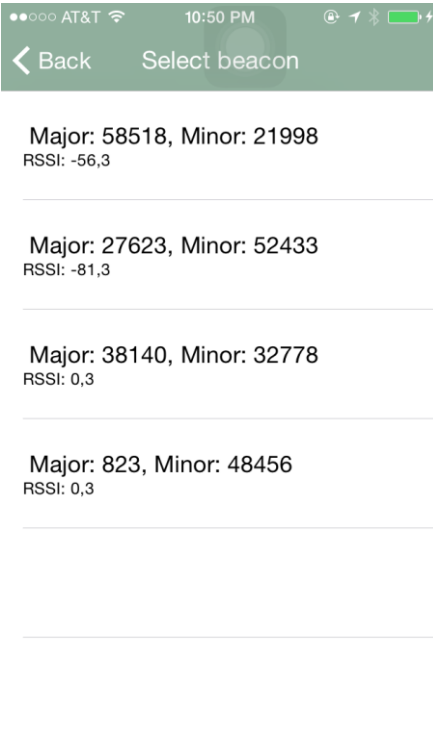


Figure 3.2 Menu of self-developed iBeacon application

3.1.1 Development using objective C

Estimote Indoor Location SDK allows real-time beacon-based mapping and indoor location. We know that building the next generation of context-aware mobile apps requires more than just iBeacon™ hardware. That's why we've built smarter software that abstracts away the difficulty of understanding proximity and position within a given space. Estimote Indoor Location is a sophisticated software solution that makes it incredibly easy and quick to map any location. Once done, you can use our SDK to visualize your approximate position within that space in real-time, in your own app. Indoor Location creates a rich canvas upon which to build powerful new mobile experiences, from in-venue analytics and proximity marketing to frictionless payments

and personalized shopping. Estimote Indoor Location works exclusively with Estimote Beacons.

When it comes to our project, we use Objective-C to develop our app to get the RSS of the beacons. The iPhone 5s acts as the receiver in our research and it is connected to a Mac book computer by a cable [28][29]. When it gets the packets from iBeacons which are in the detection range, it will display the current values of RSS both on the iPhone screen and Mac book computer. The data we collected in different situation can be used to do the channel modeling. Figure 3.3 is an example coding in Objective-C:

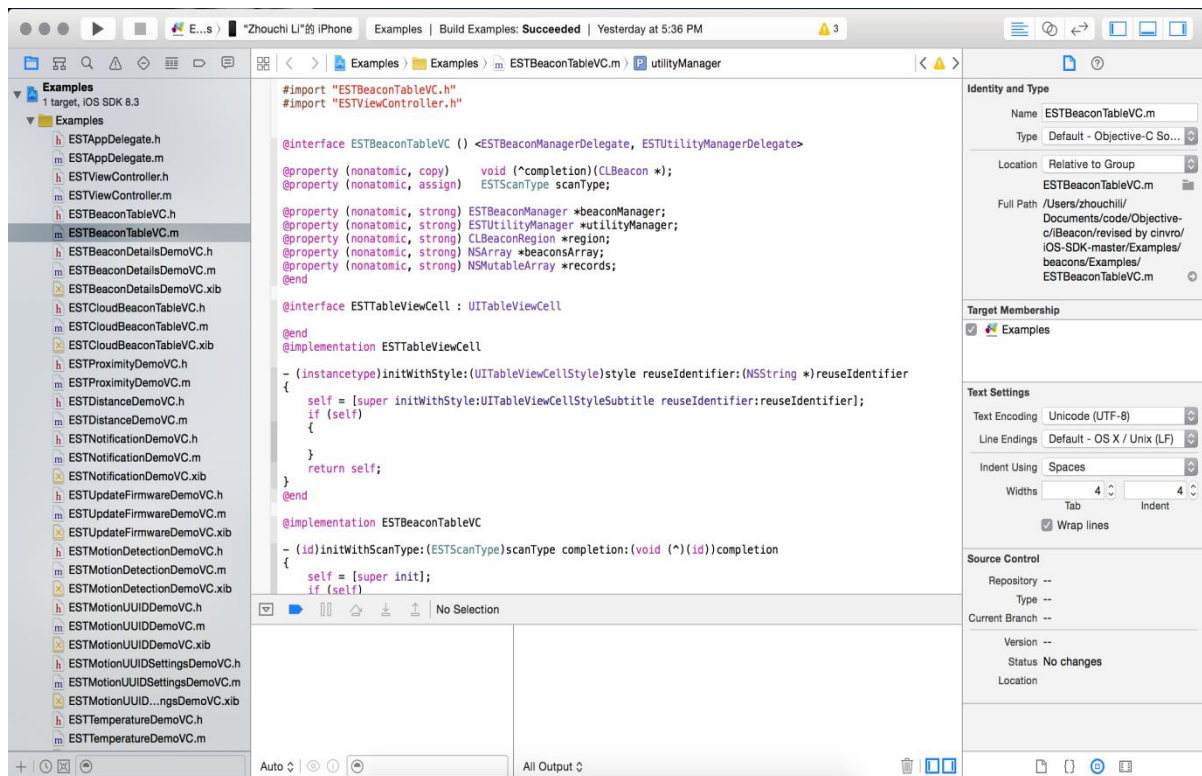
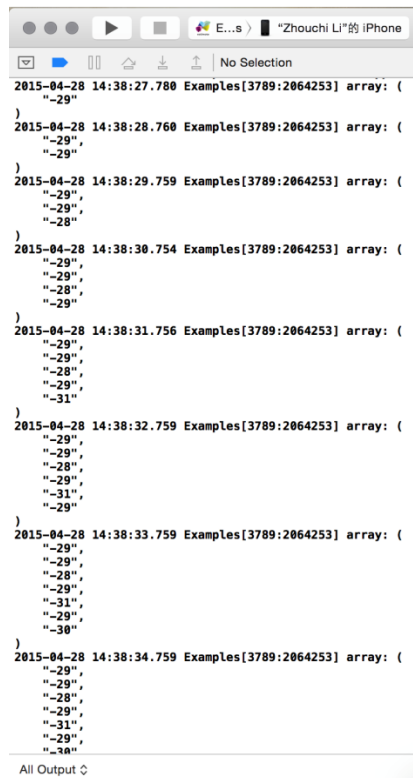


Figure 3.3 Menu of coding in Objective-C

3.1.2 Self-developed application

Figure 3.2 shows the app we have developed based on the API provided by Estimote Company. It can show the list of the beacons detected by our device and take down the RSS signal, major, minor, sequence number of the data and whatever information of beacons we want. Our need of extracting the RSS data can be satisfied by the app. Figure 3.4 shows the menu of receiving data in server.



```
2015-04-28 14:38:27.780 Examples[3789:2064253] array: (
)
2015-04-28 14:38:28.760 Examples[3789:2064253] array: (
"-29",
"-29"
)
2015-04-28 14:38:29.759 Examples[3789:2064253] array: (
"-29",
"-29",
"-28"
)
2015-04-28 14:38:30.754 Examples[3789:2064253] array: (
"-29",
"-29",
"-28",
"-29"
)
2015-04-28 14:38:31.756 Examples[3789:2064253] array: (
"-29",
"-29",
"-28",
"-29",
"-31"
)
2015-04-28 14:38:32.759 Examples[3789:2064253] array: (
"-29",
"-29",
"-28",
"-29",
"-31",
"-29"
)
2015-04-28 14:38:33.759 Examples[3789:2064253] array: (
"-29",
"-29",
"-28",
"-29",
"-31",
"-29",
"-30"
)
2015-04-28 14:38:34.759 Examples[3789:2064253] array: (
"-29",
"-29",
"-28",
"-29",
"-31",
"-29",
"-20"
)
All Output
```

Figure 3.4 Menu of receiving data in server

Figure 3.5 shows the server we built on my computer by using Python. When the app finishes receiving data of iBeacons, it will send the data to the server through the Internet. And the server will get the data and store them in a file automatically.

about the algorithms are described in my partner Zhouchi Li's master thesis ("Sensor Behavior Modeling and Algorithm Design for Intelligent Presence Detection in Nursery Rooms using iBeacon").

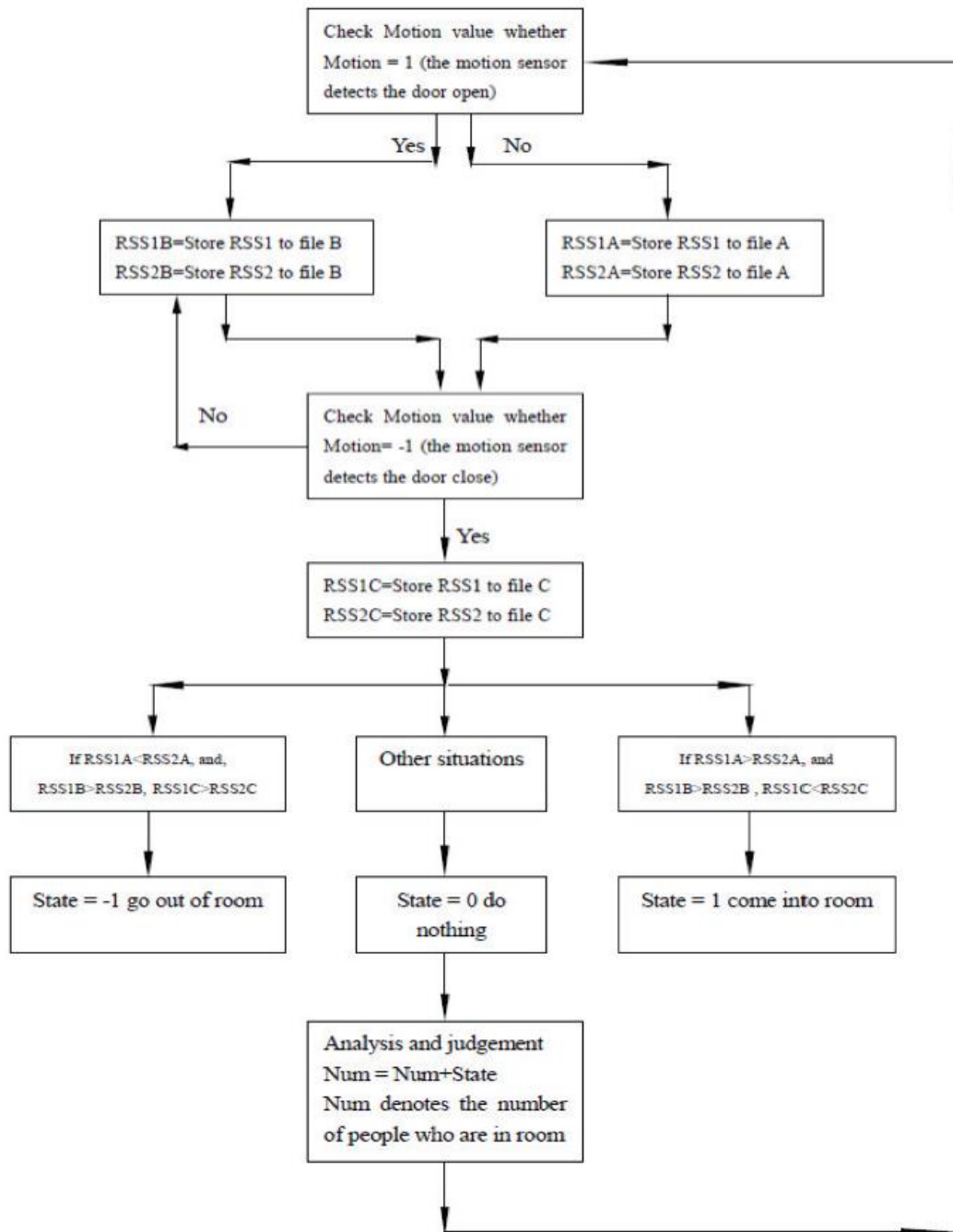


Figure 3.6 Algorithm for presence detection using 2 iBeacons

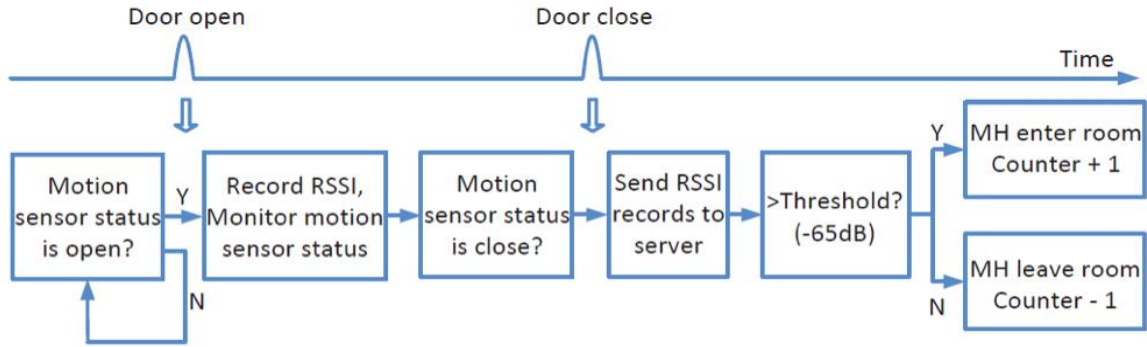


Figure 3.7 Algorithm for presence detection using 1 iBeacon

In this section we validate the proposed systems. Each previously mentioned movement has been repeated for over 500 times and the RSSI of iBeacons has been measured. By investigating the RSSI samples, we show the validity of our approach using physical observation. Apart from that, the system performance has been also recorded to help the performance comparison between double and single iBeacon approaches.

3.2.1 Double iBeacons approach

The RSSI samples for typical entering movement have been plotted in Figure 3.8. As shown in the figure, when the MH opens the door, iBeacon 1 (on outside door) provides -54dB RSSI while iBeacon 2 (on inside door) has only -61dB. With the time going, when MH goes through the door at $t = 2.5s$, both iBeacons show approximately 63.5dB RSSI. After that, when the MH gets into the room, the two RSSI curves flip over and iBeacon 2 dwells on top of iBeacon 1. As for typical leaving movement, the opposite trend can be found, which still shows that the double iBeacons approach can provide successful detection. One thing worth mentioning is that we also investigated the situation that a MH came, open the door and then closed it without entering or leaving the room. The RSSI curve for that movement has been plotted in Figure 3.9.

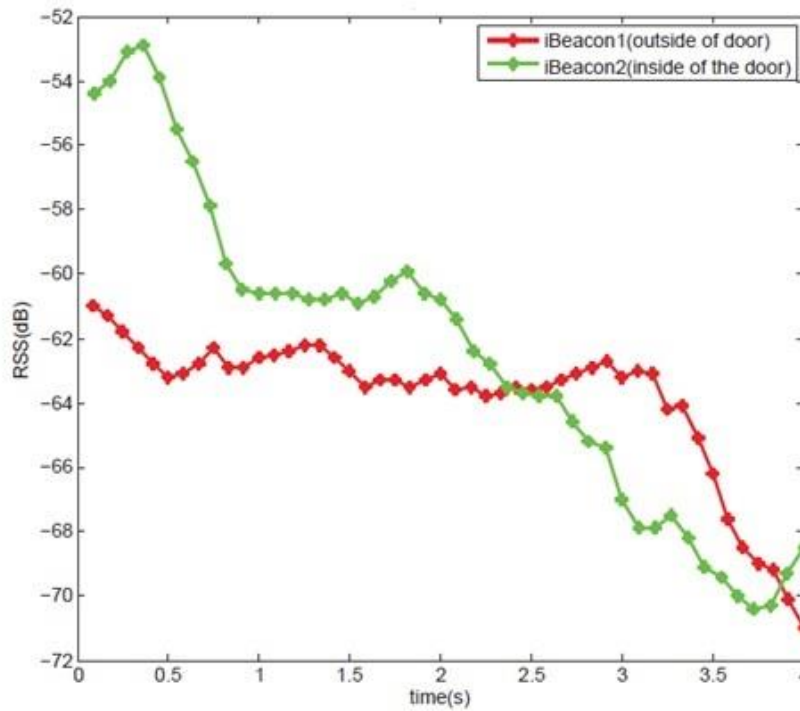


Figure 3.8 RSSI plot for double iBeacon approach, for the MH entering movement

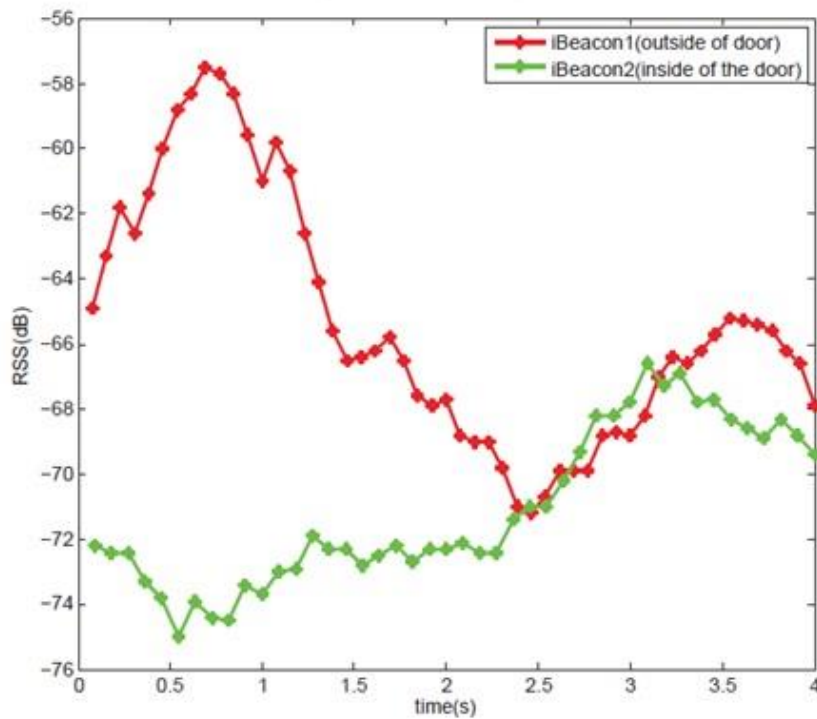


Figure 3.9 RSSI plot for double iBeacon approach, for the MH opening the door without entering/leaving

3.2.2 Single iBeacon approach

Given that the double iBeacons approach performs well, we move on to the validation of single iBeacon approach. Among our 1536 sets of empirical data, the typical cases for entering and leaving the room have been plotted in Figure 3.10. It is clear that entering the room results in higher RSSI peak due to the fact that the single iBeacon is attached to the outside of the door. When the MH is in the room, even though he/she could be close to the iBeacon, but the door lies between iBeacon and iPhone can create extra path-loss. The choice of -60dB RSSI threshold comes from the regression fitting of our empirical data, that is, we find the best fit curves for both entering and leaving movements and notice that -60dB threshold provides satisfactory detection rate of different movements. To guarantee the robustness of the single iBeacon approach, we also conduct experiments with the iPhone located at various positions. In hand, pant pocket and shirt pocket have been selected as candidate locations of the iPhone and the best fit RSSI curves have been plotted in Figure 3.10, respectively. Clearly we know that -60dB threshold works for all those iPhone positions.

It is worth mentioning that the single iBeacon approach is not able to detect the situation that the MH opens the door but neither entering nor leaving the room. Such reality shows that the single iBeacon is cost effective compared with double iBeacons approach, but is less robust against outliers.

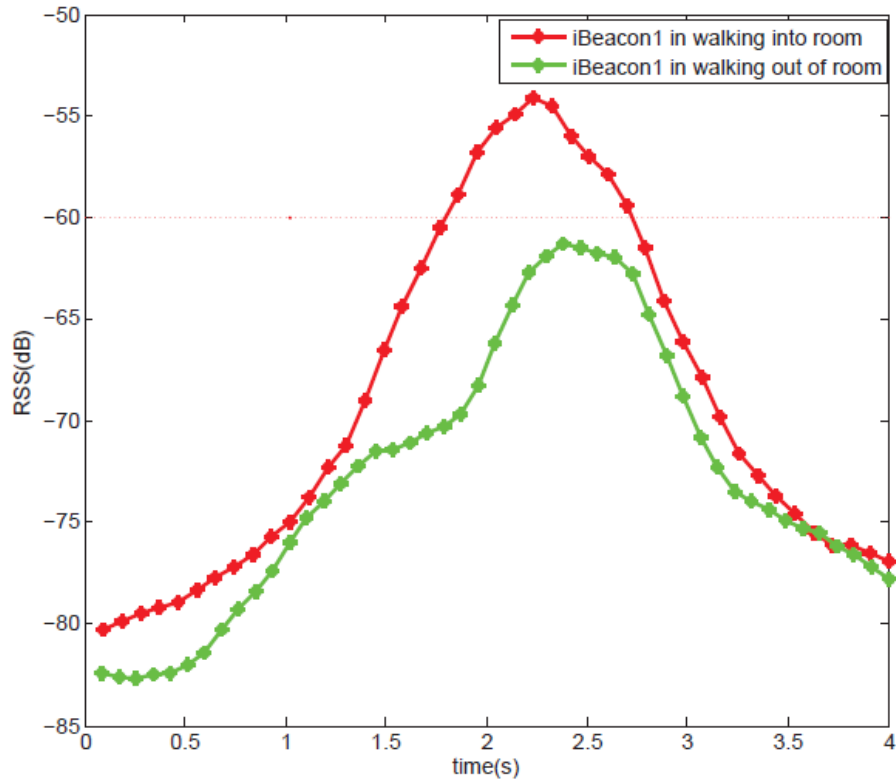


Figure 3.10 RSSI plot for single iBeacon approach, for the MH entering movement

3.2.3 Comparison

Implementation approaches	iPhone position	Detection rate	Detection rate (%)
Double iBeacon	any	1521/1521	100%
Single iBeacon	in hand	500/500	100%
	pant pocket	534/536	99.63%
	shirt pocket	500/500	100%

Table 3.1 Performance of proposed in-room presence detection approaches

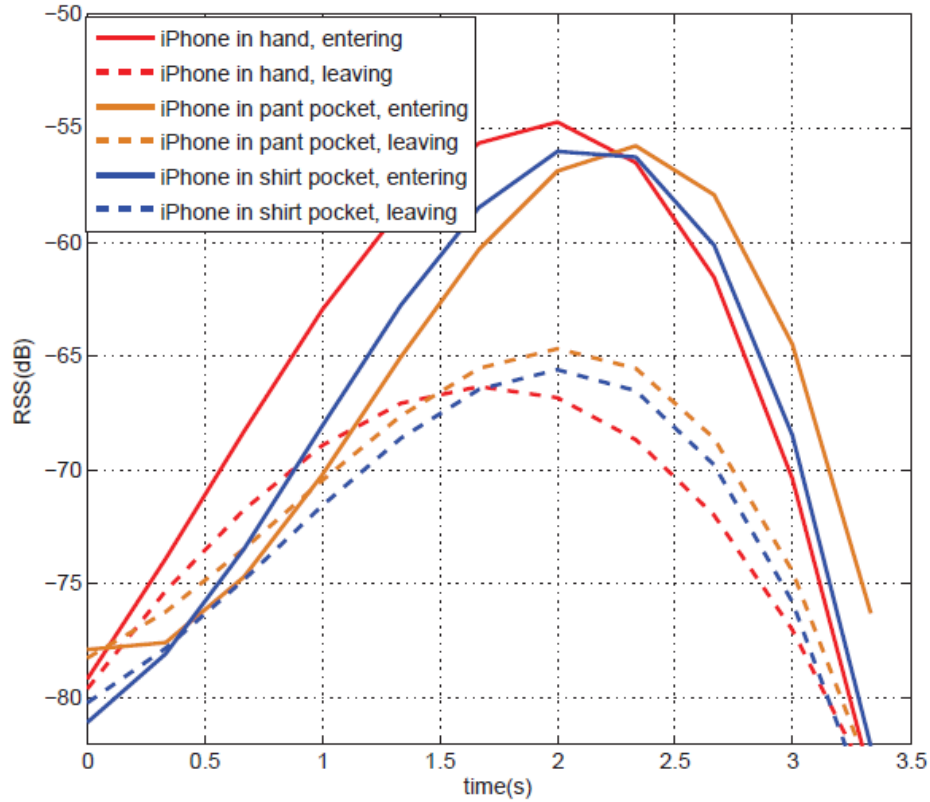


Figure 3.11 RSSI plot for various iPhone positions

At the end of this chapter, we would like to discuss the detection rates of the proposed systems. For the double iBeacons approach, we performed 521 measurements with the MH holding iPhone in hand, 500 measurements with the MH putting iPhone in pant pocket and another 500 measurements with iPhone in shirt pocket. For all these measurements, the double iBeacons approach is able to correctly detect the in-room presence. As for single iBeacon approach, we have 536 measurements with the MH holding iPhone in hand, 500 measurements with the MH putting iPhone in pant pocket and another 500 measurements with iPhone in shirt pocket. For the pant pocket iPhone position we have 2 mis-detections, while for in hand and shirt pocket cases the detection rates are all 100% (shown in table 3.1). With such experimental results, we would like to claim that both approaches work well.

Chapter 4

Methodology and discussion for in-room Localization using iBeacon

At the beginning of this chapter, we firstly derive the empirical path-loss model and construct Estimote iBeacon path-loss model [23]. The comparison demonstrates a fact that the empirical model shows a lower distance measure error (DME) and better performance. Secondly, we simulate the in-room environment to compute Cramer-Rao low bound of location error both in 2D and 3D scenarios to observe the influence of estimation of location error under different deployment patterns of iBeacons and try to find an optimal method to deploy iBeacons [24]. Specifically, we compare the cumulative distribution functions (CDF) of the CRLB in three different deployment patterns as well as different number of iBeacons to make our conclusions.

4.1 Path-loss modeling

In this section, we introduce our data collecting system based on which we collect RSS data and derive the empirical path-loss model. Then we compare the performance of that model and existing iBeacon model by the CDF of DME to reach the conclusion that our empirical path-loss model is more reliable. This model will be used in the simulations in the rest parts.

4.1.1 RSSI data collection system

The iBeacons produced by Estimote Company can provide us much information we need

such as RSS, broadcasting interval, minor and major values and even motion sensor. However, the existing app from Estimote Company do not allow us to collect data directly from iPhone which means large samples are impossible and we can only collect data by hand. To solve this problem, we decide to develop our own app.

We use Objective-C to develop our app to get the RSS of the beacons. The iPhone 5s acts as the receiver in our research and it is connected to a Mac book computer by a cable. When it gets the packets from iBeacons which are in the detection range, it will display the current values of RSS both on the iPhone screen and Mac book computer. The data we collected in different situation can be used to do the channel modeling.

The achievements of our developing own app:

1. Connect with certain iBeacon.
2. Set the UUID, major and minor fields of iBeacon.
3. Collect and store the RSS information.
4. Extract the RSS data from iphone. This makes the data more reliable compared

with those collected by hand, and also make the samples much larger.

4.1.2 Modeling and validation

Before we start to collect data, we need to validate the measurement environment can use the IEEE 802.11 model or not. Since RSS is the most important factor in this project, the path-loss model must be established [30]. We do linear match fitting with different iBeacon data collected by our app to try to find out the best path-loss model of iBeacon. Distance measure error (DME) is the criterion we use to compare the performance of each model. The CDF of DME of different can tell us which model is better.

With the data we collected, here is the path-loss model in LOS situation from Matlab.

After linear match fitting with the RSS, we have figure 4.1 which shows us the power gradient and the pass-loss in first meter.

In order to find out how Estimote Company measure the distance by iBeacon, we recorded the RSS data shown in Estimote app when the app indicated we were on the boundaries of first and second circles(distances are 1m and 5m). With the RSS data of these two points, we can figure out the path-loss model using by iBeacon. We have two path-loss models for each iBeacon coming from Estimote Company and our own app, we can see that there some differences between these two models.

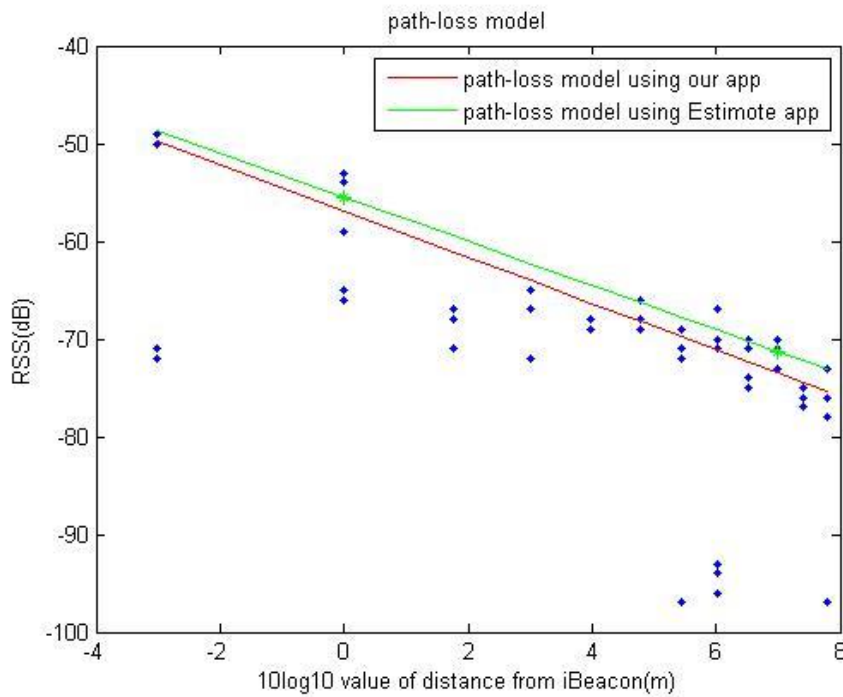


Figure 4.1 Two path-loss models comparison

With the data we collected by mint iBeacon, we can find out the estimate distance by using the RSS data and path-loss model. Since the two models are both like

$$RSS = P_0 + 10 \alpha \log \hat{d}$$

We can have

$$\hat{d} = 10^{\frac{RSS-P_0}{10\alpha}}$$

Then the DME can be shown as

$$DME = |d - \hat{d}|$$

where d is the real distance we have in measurement. We calculate the DME for each point data we have and then compute the CDF of the DME to compare the performance of these two models, the CDF of mint iBeacon is shown in figure 4.2.

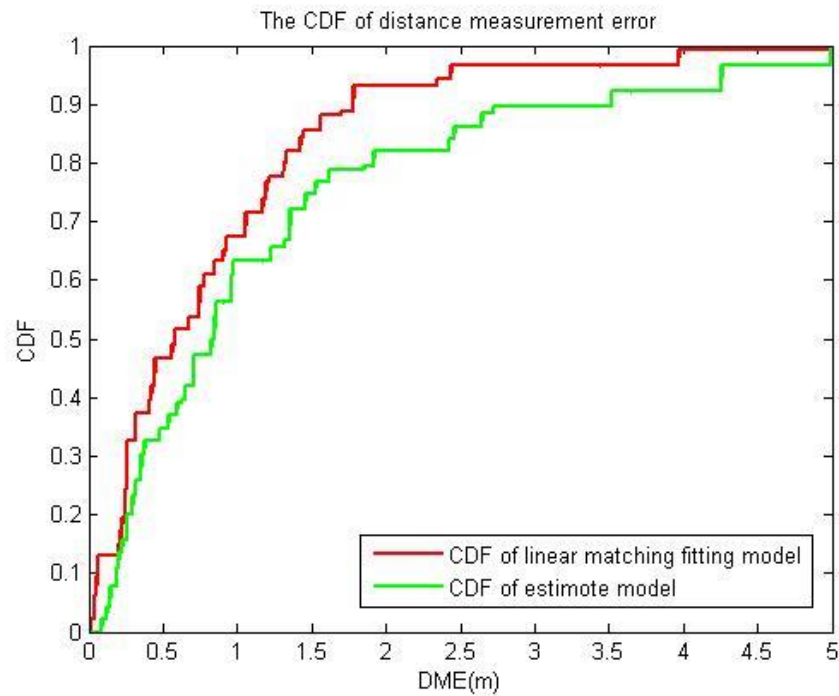


Figure 4.2 Comparison of cumulative distribution functions of distance measurement error in two models

From figure 4.2 we can see that the red one is on the left side of green one which means our path-loss model coming from linear match fitting has less error in the same DME range. In a word, the linear match fitting path-loss model shows a better performance.

4.1.3 Discussion of path-loss modeling

In this section, different iBeacons have different path-loss model which may be caused by shadow fading or measurement error. However, after comparing the CDF of DME, our model coming from linear matching shows a better performance, using our model may have a better distance judgement. The overall two path-loss models are shown in table 4.1, where $\sigma_{sf}(m)$ means the mean of shadow fading using each model.

Item	iBeacon model			Empirical path-loss model		
	$L_0(\text{dB})$	α	$\sigma_{sf}(\text{dB})$	L_0	α	$\sigma_{sf}(\text{dB})$
iBeacon1	-54.8995	2.5214	3.2013	-55.3555	2.4674	3.5773
iBeacon2	-55.5000	2.2540	4.2992	-56.8918	2.3689	3.0501
iBeacon3	-52.5628	2.7693	4.1208	-56.1283	2.5387	3.1099

Table 4.1 Parameters of two different path-loss models

Based on the models, we also calculate the DME of each model to decide which one owes a better performance, the comparison results are shown in table 4.2, where $m_e(m)$ means the mean of DME using each model and $\sigma_e(m)$ means the standard variance of DME using each model.

Item	iBeacon model		Empirical path-loss model	
	$m_e(m)$	$\sigma_e(m)$	$m_e(m)$	$\sigma_e(m)$
iBeacon1	0.8716	1.1819	0.8771	1.2179
iBeacon2	1.6717	4.9553	1.0788	1.4071
iBeacon3	0.1739	2.0837	0.9872	1.9240

Table 4.2 Distance measurement error comparison of two models

4.2 Scenarios and algorithms of in-room Localization

Ranging-based localization is the task of identifying the positions of a network of nodes based on estimates of the distances between them, called range estimates. In many ways, radio signal strength (RSS) is an ideal modality for range estimation in wireless networks because RSS information can be obtained at no additional cost with each radio message sent and received [31][32]. The simplicity of RSS is especially appealing for the localization in wireless sensor networks because of their cost, size, and power constraints, despite the fact that RSS may yield very noisy range estimates. In this section, we empirically introduce the main methodology of RSS-based localization such we can have an overview of in-room localization using iBeacon.

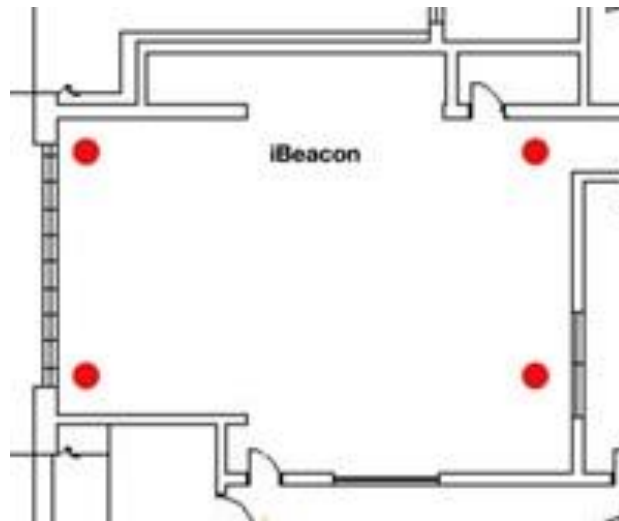


Figure 4.3 Scenario for in-room localization

Figure 4.3 shows the main scenario for in-room localization that there are 4 iBeacons in each corner of a room. This is a typical scenario that we usually consider it as our first choice. It is very similar to Wi-Fi localization if we regard the iBeacons as access points.

To the localization in this room, we record the RSS data from all these 4 iBeacons, from each iBeacon RSS data we can calculate a distance range based on the path-loss model we construct in section 4.1[33][34][35]. Then we use that distance range as radius range and take the location of each iBeacon as a center to draw circles. The overlap area shown in red shows the possible location we locate by iBeacon, shown in figure 4.4.

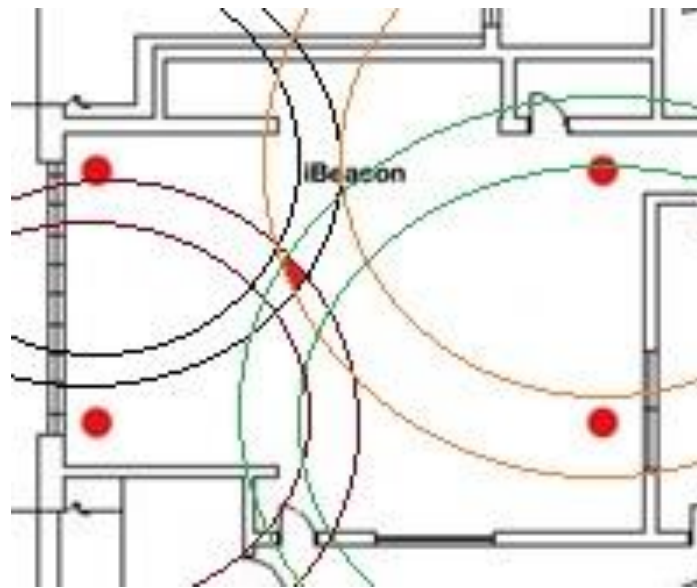


Figure 4.4 Scenario of RSS ranging localization

4.3 Methodology for performance evaluation

In this section, we firstly introduce the scenarios we define to evaluate the performance of using iBeacon in localization. Then based on Matlab, we simulate the in-room localization environment and calculate the estimation of location error (CRLB) to show the effects of different deployment patterns and different iBeacon numbers [25][36][37]. Furthermore, we promote our model from 2D to 3D scenario and figure out the estimation of location error to present the feasibility in this case.

4.3.1 Scenarios for performance evaluation

In order to compare the performance of different localization methods, in this paper we use Cramer-Rao low bound of the location error standard deviation as the assessment criterion. According to the conclusion given in [25], we know how to calculate the location error standard deviation. We use Matlab simulation to obtain the theoretic results.

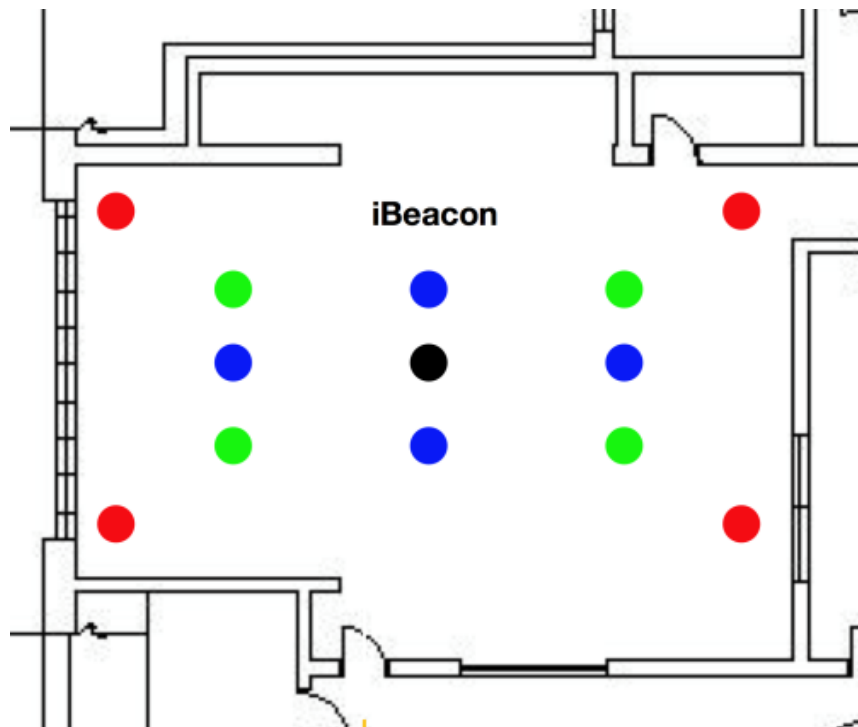


Figure 4.5 Scenarios of different deployment methods

Since we want find the most efficient way of localization, different deployment methods are introduced, based on which we can compare and make conclusion. It is easy to know that more iBeacons stands for more localization accuracy, but what we pursue is how to reach the highest accuracy with special given iBeacons, so there are 3 scenarios we simulated shown in figure 4.5 in 3 different colors. In the first scenario, there are four iBeacons in the four corners of the room and another one in the middle of the room. As

for the second scenario, there are four iBeacons in the four corners of the middle area of the room and also another one in the middle of the room. To the last scenario, it is almost as the same as the second one, except for the rotation of 45 degrees of the four iBeacons deployed in the middle area, which means we rotate the square formed by the second deployment method with 45 degrees into a new deployment pattern.

4.3.2 Localization error estimation of deployment patterns

As we discussed before, there are 3 scenarios we analyze and compare in order to evaluate the feasibility and effectiveness. From the Matlab we have such conclusions. The simulation conditions for location error analysis are as follows:

$P_r(0) = 160W = 52dBm$, and $\alpha = 2.4583$ which is the mean of the α values of empirical path-loss model derived in section 4.1.3 (shown in Table 4.1).

In the first scenario, we assume that there are five APs installed in a building with their coordinates being AP 1 (15m, 15m), AP 2 (15m, -15m), AP 3 (-15m, -15m), AP 4 (-15m, 15m), and AP 5 (0.1m, 0.1m) [25]. If an MS at a given location receives signals from these APs, its position can be determined by triangulation or least square estimation. The simulation result is shown figure 4.6 to figure 4.8.

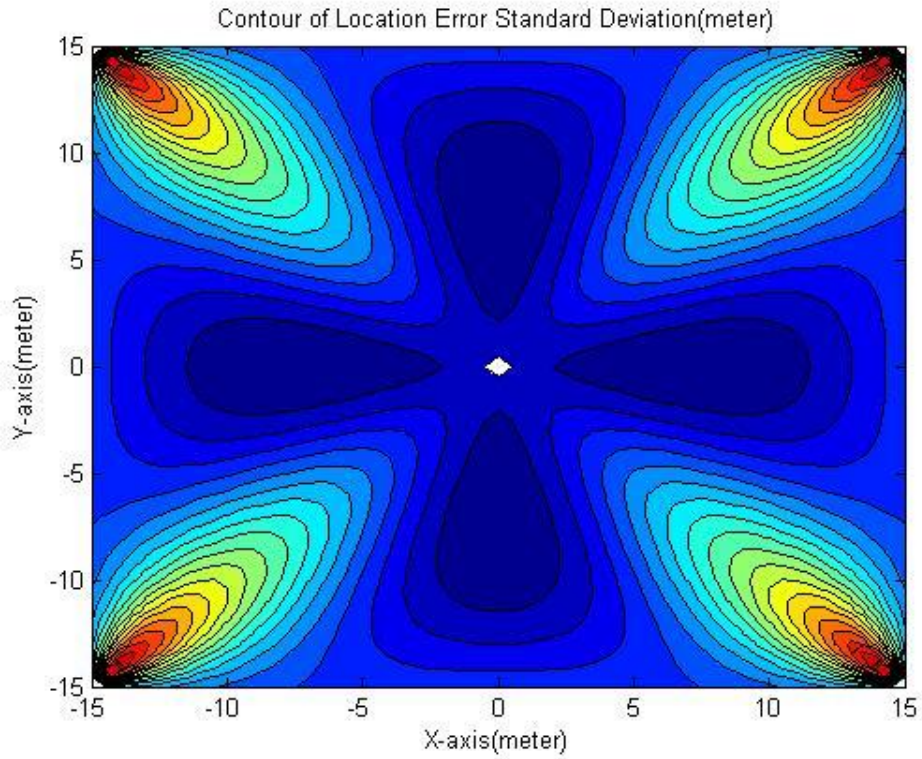


Figure 4.6 Contour of estimate location error in 2D in scenario 1

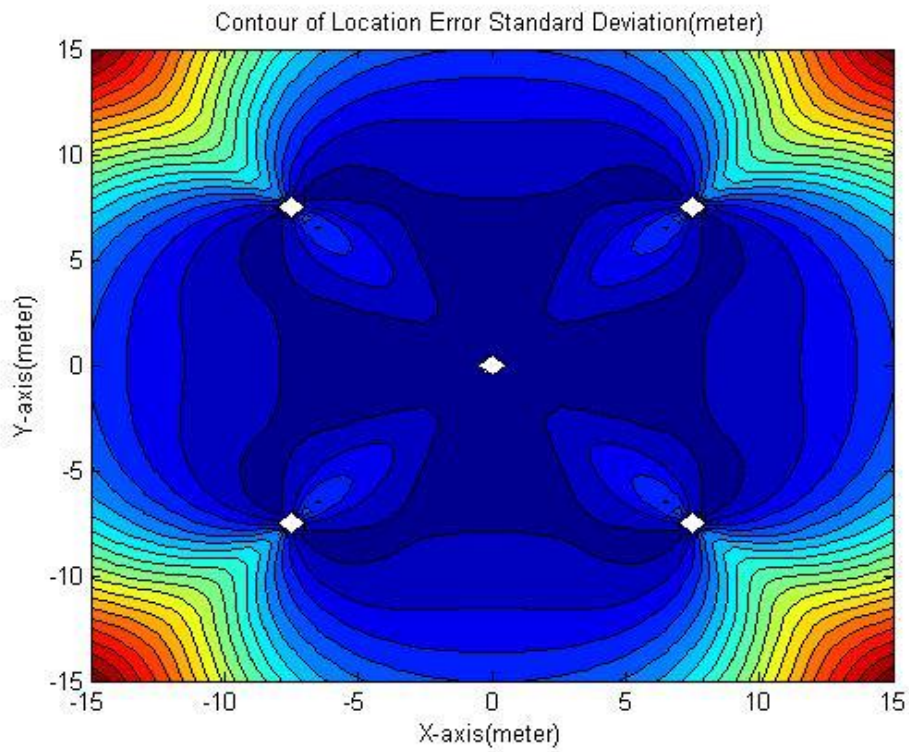


Figure 4.7 Contour of estimate location error in 2D in scenario 2

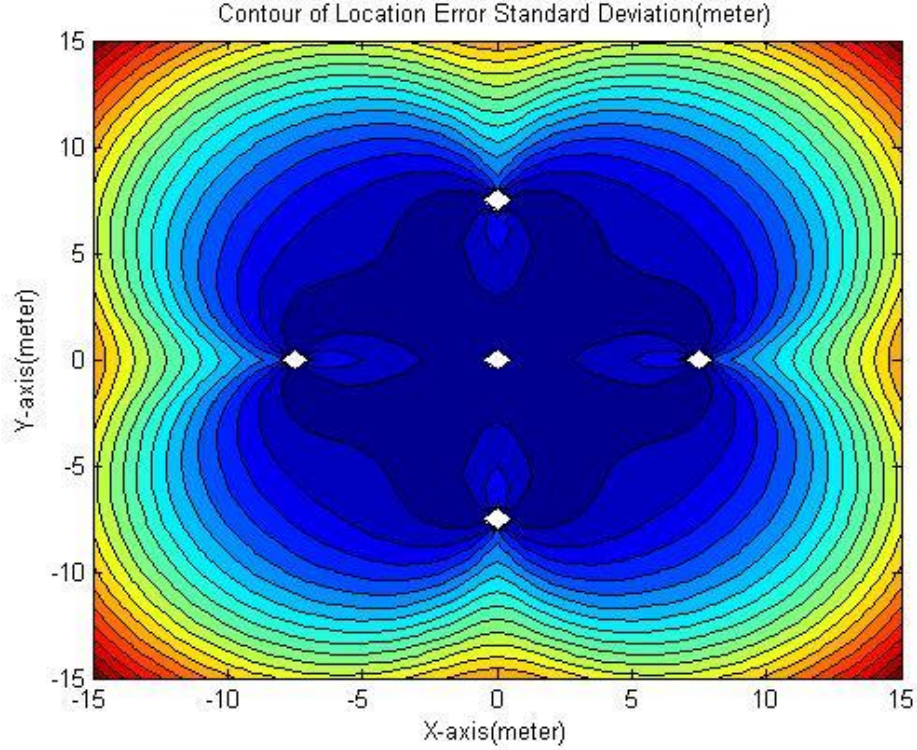


Figure 4.8 Contour of estimate location error in 2D in scenario 3

Then we move the four iBeacons from four corners to the middle area of the room to reach the second scenario and also make such type figure. When we come to the last scenario, we just do a rotation of 90 degrees with the four iBeacons in the middle and reach the result.

4.3.3 CRLB for performance evaluation in 3D.

Since the nursery room is a cube in reality, we extend the formula and simulation conditions from 2D to 3D. Z axis is introduced into the original $x \times y$ plane and we also move the fifth iBeacon from the middle of ground up to the middle of the roof.

Based on the well-known path-loss model [25], we have:

$$P(r) [\text{dBm}] = P(r_0) [\text{dBm}] - 10\alpha \log\left(\frac{r}{r_0}\right)$$

Transfer it into 3D coordinate form:

$$dP_i(x, y, z) = -\frac{10\alpha}{\ln 10} \left(\frac{x - x_i}{r_i^2} dx + \frac{y - y_i}{r_i^2} dy + \frac{z - z_i}{r_i^2} dz \right)$$

We can also write it into a vector form, like:

$$d\vec{P} = \vec{H} \cdot d\vec{r}$$

Where,

$$d\vec{P} = \begin{bmatrix} dP_1 \\ dP_2 \\ \vdots \\ dP_N \end{bmatrix}, d\vec{r} = \begin{bmatrix} dx \\ dy \\ dz \end{bmatrix}, \vec{H} = \begin{bmatrix} -\frac{10\alpha}{\ln 10} \frac{x - x_1}{r_1^2} & -\frac{10\alpha}{\ln 10} \frac{y - y_1}{r_1^2} & -\frac{10\alpha}{\ln 10} \frac{z - z_1}{r_1^2} \\ -\frac{10\alpha}{\ln 10} \frac{x - x_2}{r_2^2} & -\frac{10\alpha}{\ln 10} \frac{y - y_2}{r_2^2} & -\frac{10\alpha}{\ln 10} \frac{z - z_2}{r_2^2} \\ \vdots & \vdots & \vdots \\ -\frac{10\alpha}{\ln 10} \frac{x - x_N}{r_N^2} & -\frac{10\alpha}{\ln 10} \frac{y - y_N}{r_N^2} & -\frac{10\alpha}{\ln 10} \frac{z - z_N}{r_N^2} \end{bmatrix}$$

Then, deriving in the same method [25], the estimation of location error can be calculated as:

$$\text{cov}(d\vec{r}) = \sigma_p^2 (\vec{H}' \vec{H})^{-1} = \begin{bmatrix} \sigma_x^2 & \sigma_{xy}^2 & \sigma_{xz}^2 \\ \sigma_{yx}^2 & \sigma_y^2 & \sigma_{yz}^2 \\ \sigma_{zx}^2 & \sigma_{zy}^2 & \sigma_z^2 \end{bmatrix}$$

$$\sigma_r = \sqrt{\sigma_x^2 + \sigma_y^2 + \sigma_z^2}$$

Where σ_p is considered as 2.5 [25] in the simulations.

Due to plotting of a 4D figure is impossible, we give figure 4.9 in a particular height.

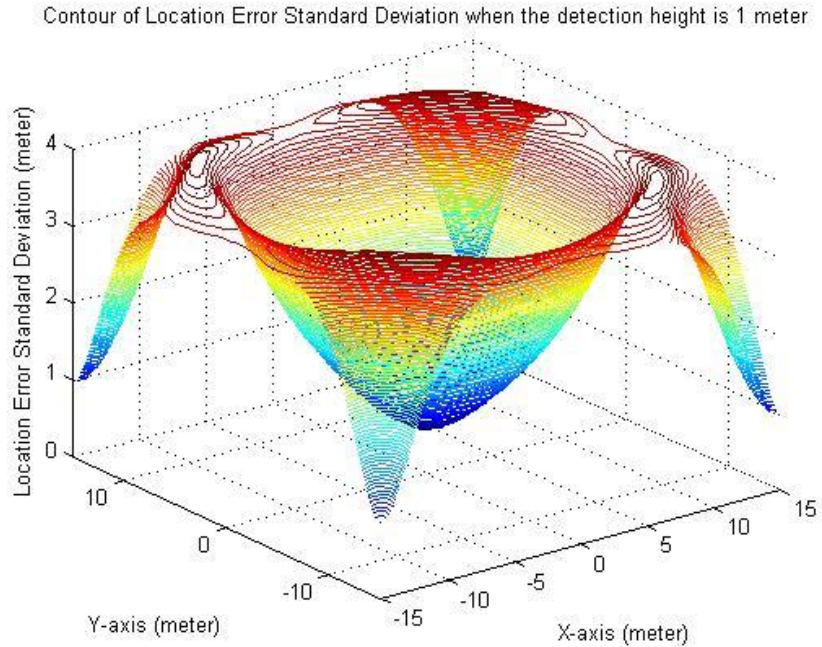


Figure 4.9 Contour of estimate location error in 3D

4.4 Effect analysis of different deployment methods

In this section, we compare the CDF of the error in three different deployment patterns to present the results of our in-room deployments. Later on, we also observe the influence of number of iBeacon by simulations in the same conditions to show the most efficient deployment method.

4.4.1 Effect of different deployment patterns.

In order to observe the performance of 3 different scenarios directly, we calculate the CDF of estimation of location error and compare them. In fig. we can see that the deployment with four iBeacons in the middle area has the best performance, this is probably because in this scenario it owes the highest overlap rate of coverage area, which means that most part of the room can be located by 2 or more iBeacons and results in the

highest accuracy.

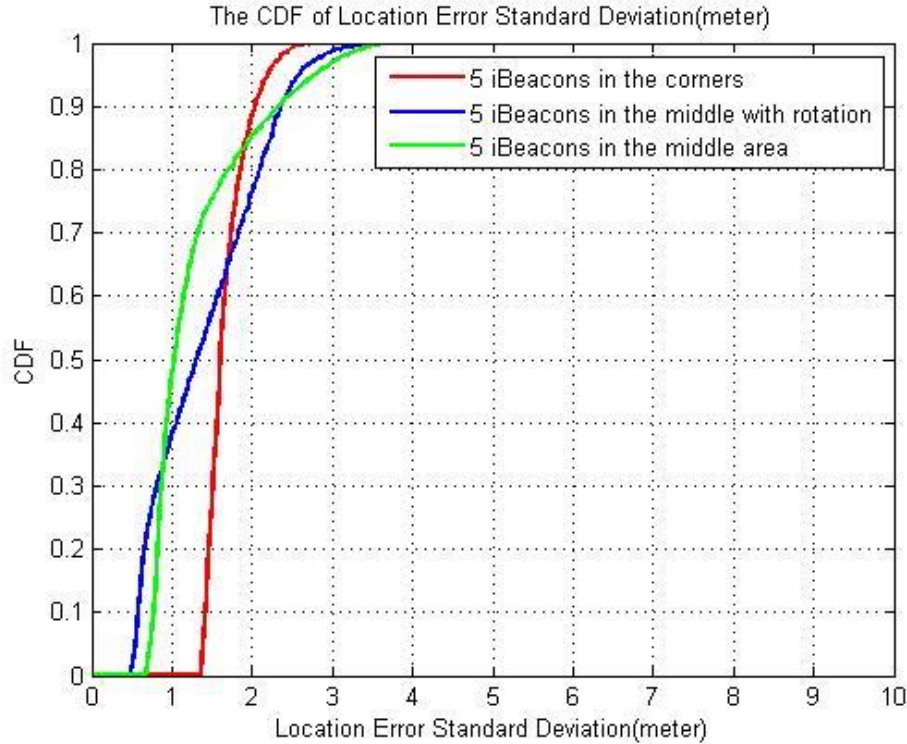


Figure 4.10 Comparison of cumulative distribution functions of CRLB in 3 different deployment patterns

Apart from that, based on the figure 4.6 to figure 4.8 we present before, we also calculate the means and variances of CDF of the location estimation error in the different scenarios. From the figure we can claim that 5 iBeacons in the middle area performs best (green line in figure 4.10). The comparison is in table 4.3.

Parameters	5 iBeacons in corners	5 iBeacons in the middle area	5 iBeacons in the middle area with rotation
mean	1.6755m	1.2935m	1.4023m
Standard variance	0.2584m	0.6471m	0.7001m
90%error bound	2.1223m	2.3312m	2.3547m

Table 4.3 Comparison of CRLB in 3 different deployment patterns

4.4.2 Effect of different number of iBeacons

In addition to the different deployment patterns, it is more reasonable to take into account the number of iBeacon. With the same simulation conditions in Matlab, we conclude the performance with 3, 4 and 5 iBeacons in the same environment. The simulations can be viewed in figure 4.11 to figure 4.13.

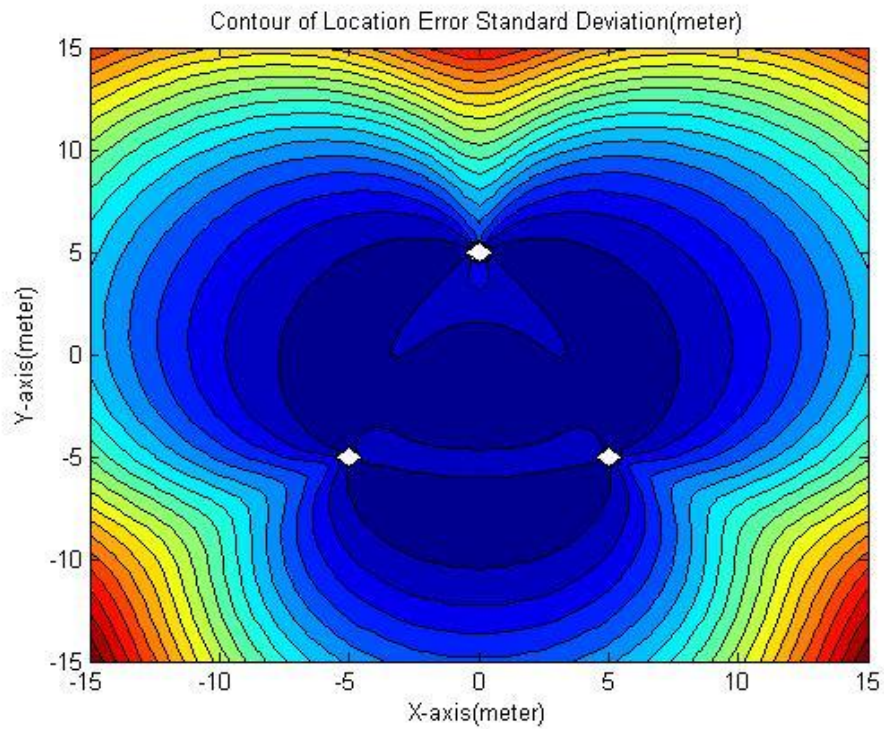


Figure 4.11 Contour of estimate location error of 3 iBeacons

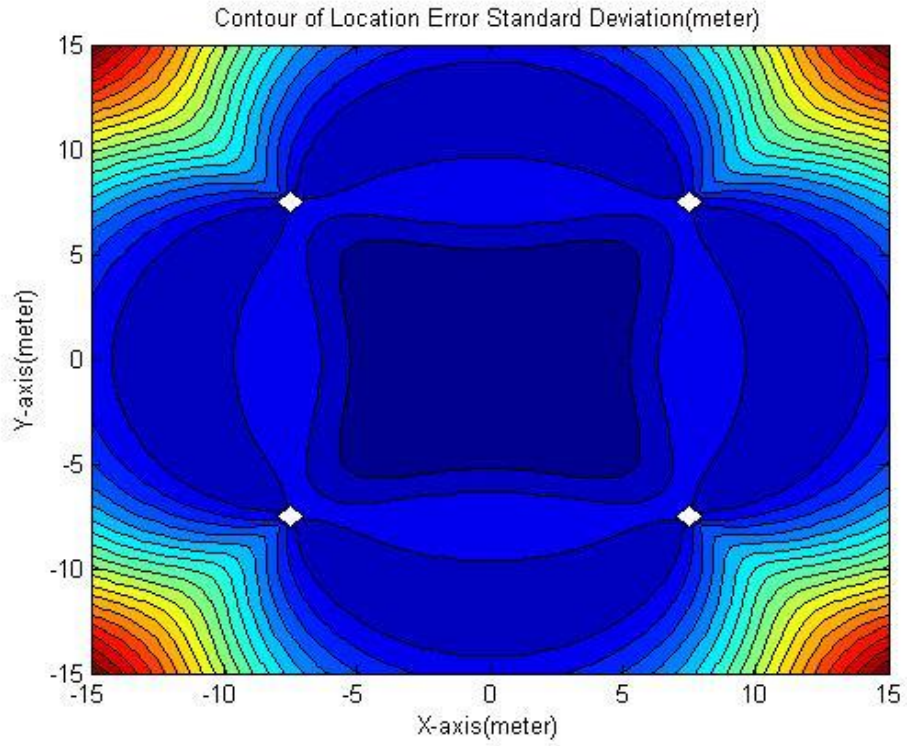


Figure 4.12 Contour of estimate location error of 4 iBeacons

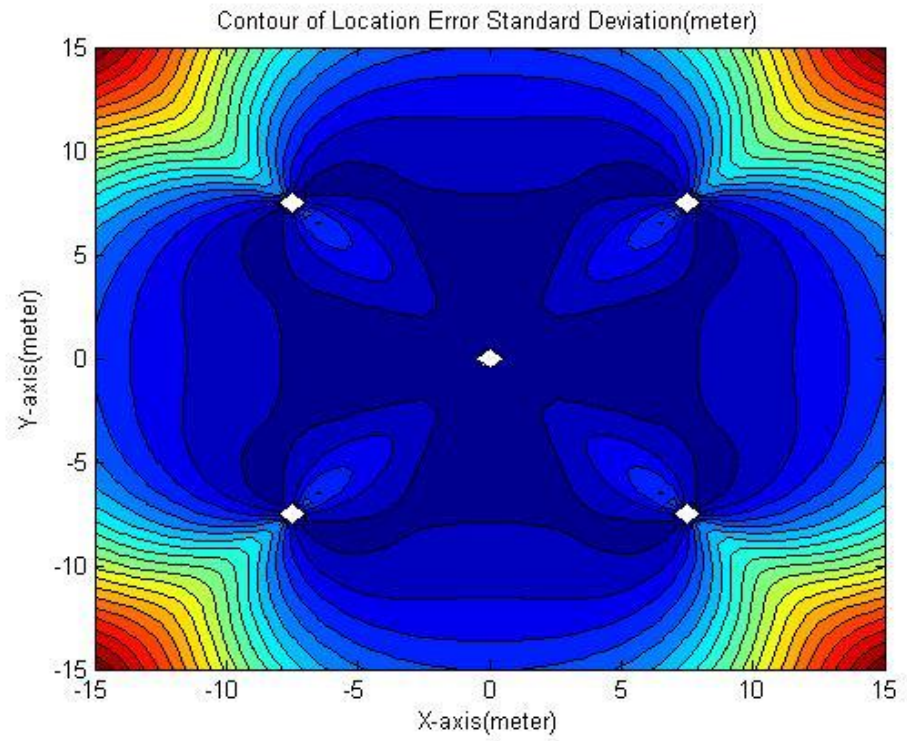


Figure 4.13 Contour of estimate location error of 5 iBeacons

Above are the error estimation results with 3,4 and 5 iBeacons in the middle area since we have already certified that the deployment in the middle owes the best performance. In addition, we can still calculate the CDF of the location estimation error to compare them and reach a conclusion, shown in figure 4.14.

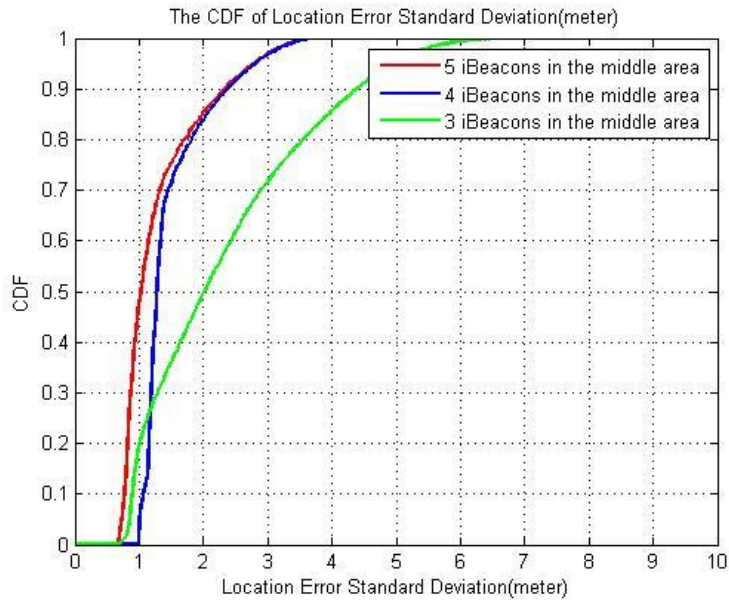


Figure 4.14 Comparison of cumulative distribution functions of CRLB in different number of iBeacons

Obviously, 5 iBeacons owes the best performance, however, we can find that the improvement from 3 iBeacons to 4 iBeacons is significant while the improvement from 4 iBeacons to 5 iBeacons is negligible. So we can assert that the deployment with 4 iBeacons in the middle area contains the highest efficiency. The overall performance is concluded in table 4.4.

Parameters	5 iBeacons	4 iBeacons	3 iBeacons
mean	1.2935m	1.5060m	2.3332m
Standard variance	0.6471m	0.5536m	1.3401m
90%error bound	2.3312m	2.3392m	4.4107m

Table 4.4 Comparison of CRLB in different number of iBeacon

Chapter 5

Performance evaluation for in-room localization technology using iBeacon

In this chapter, we analyze the Cramer-Rao Lower Bound (CRLB) of localization using Received Signal Strength (RSS) considering detection probabilities and variable shadow fading. This analysis has a dual purpose [38]. Firstly, the properties of the bound on localization error may help to design efficient localization algorithm. For example, utilizing one of the properties, we propose a way to define the most efficient deployment scheme based on different access points range and room size which is shown to perform better than random deployment. Secondly, it provides suggestions for deploying access points or iBeacons by revealing error trends associated with the system deployment methods. In both cases, simulation results in Matlab are presented in order to support our claims.

Among all the chapters we discussed before, we assume the probability that someone is covered by access points or iBeacons is always 1 and shadow fading is a constant. However, in reality we need to take into account the fade margin and variable shadow fading (decided by distance). So we organize this chapter as follow: In section 5.1, we explain the definition of shadow margin and analyze it in numerical form, then derive the coverage possibility. In section 5.2, we introduce the main algorithms of CRLB and combine this CRLB with the coverage probability. Meanwhile, we also use variable shadow fading rather than constant shadow fading into the CRLB and give figures to show the simulation results in Matlab. As for section 5.3, we illustrate the analysis results

in figures and give conclusions.

5.1 Coverage possibility

For $\gamma\%$ coverage, the base station should have an additional fade margin of F_σ that [11]:

$$1 - \gamma = \int_{F_0}^{\infty} f_{SF}(x) dx = 0.5 \operatorname{erfc} \left(\frac{F_\sigma}{\sqrt{2}\sigma} \right)$$

The fade margin is the additional signal power that can provide a certain additional fraction of the locations at the edge of a cell (or near the fringe areas) with the required signal strength. Thus, for computing the coverage with certain assurance for coverage, we first determine the fade margin using the variance of the shadow fading. Then we employ the following equation to calculate the coverage [11]:

$$L_p = L_0 + 10\alpha \log d + F_\sigma$$

where F_σ is the fade margin associated with the path loss to overcome the shadow fading component. This fading margin can be applied by increasing the transmit power and keeping the cell size the same, or reducing the cell size by setting a higher RSS threshold for making a handoff. For commonly employed probabilities of coverage such as 95 or 90%, we can use the following formulas to compute the fade margins.

We note that the location variability component X (in dB) in this case is a zero mean Gaussian random variable [39][38]. Here we use σ to denote the standard variance of the shadow fading and chose $1 - \gamma \% = 10\%$, that is, 90% of the locations will have a fading component smaller than the tolerable value. Using the complementary error function and

Matlab, we can determine the value of $F\sigma$ as the solution to the equation $0.1 = 0.5 \operatorname{erfc}(F\sigma/\sigma)$ [11]. Due to the fact that with the distance increased, $F\sigma$ will become smaller, we can then calculate the distance which is able to satisfy the $F\sigma$ for a certain possibility, like [41][42]:

$$d = 10^{\frac{L_p - L_0 - F\sigma}{10\alpha}}$$

To show the result directly in figure, we suppose there is an access point (iBeacon) in a corner of a room, then compute the coverage possibility based on the distance. Figure 5.1 shows the result:

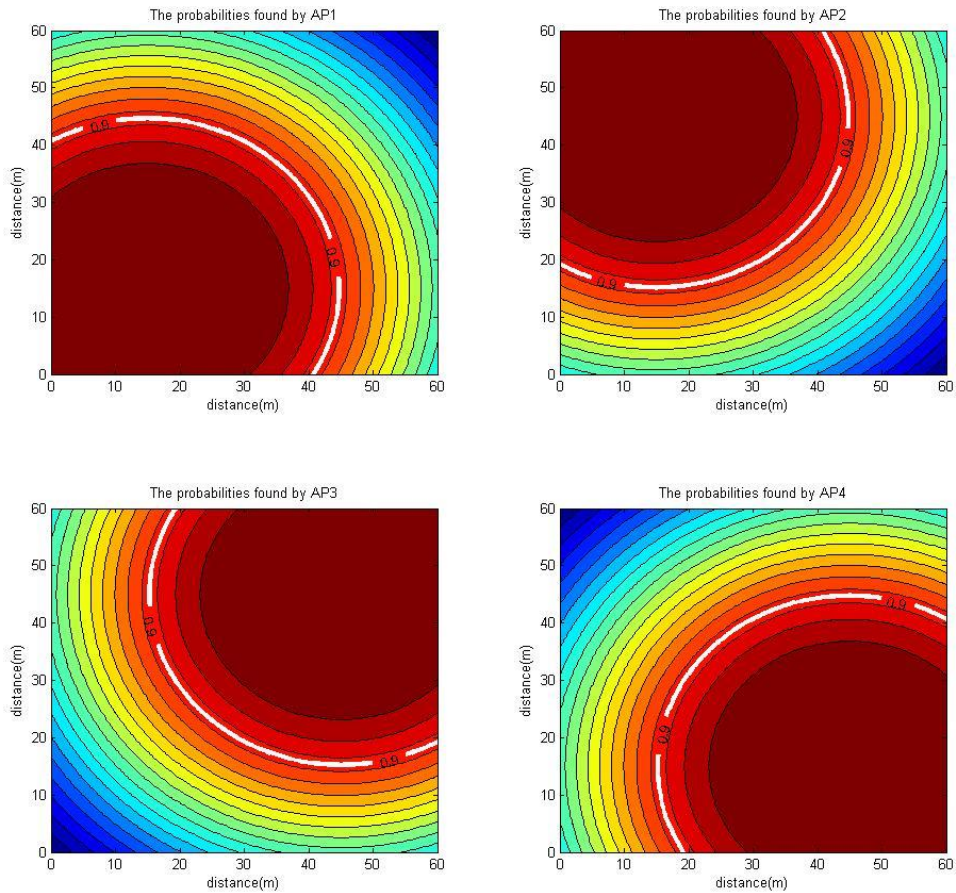


Figure 5.1 Relationships between coverage possibility and distance

The white line shows the distance which can satisfy the condition of offering a 90% shadow fading margin.

Apart from that, now the scenario is we put 4 access points (APs) or iBeacons in each corner of a room, it is reasonable to think about the detection probabilities by different number of APs. For different number of Aps, we introduce these formulas to calculate [43][44][45]:

If there is no access point covered:

$$P_0 = (1-P_{C1}) \times (1-P_{C2}) \times (1-P_{C3}) \times (1-P_{C4})$$

If there is 1 access Point covered:

$$P_{11} = P_{C1} \times (1-P_{C2}) \times (1-P_{C3}) \times (1-P_{C4})$$

$$P_{12} = P_{C2} \times (1-P_{C1}) \times (1-P_{C3}) \times (1-P_{C4})$$

$$P_{13} = P_{C3} \times (1-P_{C1}) \times (1-P_{C2}) \times (1-P_{C4})$$

$$P_{14} = P_{C4} \times (1-P_{C1}) \times (1-P_{C2}) \times (1-P_{C3})$$

$$P_1 = P_{11} + P_{12} + P_{13} + P_{14}$$

If there are 2 access Points covered:

$$P_{21} = P_{C1} \times P_{C2} \times (1-P_{C3}) \times (1-P_{C4})$$

$$P_{22} = P_{C1} \times P_{C3} \times (1-P_{C2}) \times (1-P_{C4})$$

$$P_{23} = P_{C1} \times P_{C4} \times (1-P_{C2}) \times (1-P_{C3})$$

$$P_{24} = P_{c2} \times P_{c3} \times (1 - P_{c1}) \times (1 - P_{c4})$$

$$P_{25} = P_{c2} \times P_{c4} \times (1 - P_{c1}) \times (1 - P_{c3})$$

$$P_{26} = P_{c3} \times P_{c4} \times (1 - P_{c1}) \times (1 - P_{c2})$$

$$P_2 = P_{21} + P_{22} + P_{23} + P_{24} + P_{25} + P_{26}$$

If there are 3 access Points covered:

$$P_{31} = P_{c1} \times P_{c2} \times P_{c3} \times (1 - P_{c4})$$

$$P_{32} = P_{c1} \times P_{c2} \times P_{c4} \times (1 - P_{c3})$$

$$P_{33} = P_{c1} \times P_{c3} \times P_{c4} \times (1 - P_{c2})$$

$$P_{34} = P_{c2} \times P_{c3} \times P_{c4} \times (1 - P_{c1})$$

$$P_3 = P_{31} + P_{32} + P_{33} + P_{34}$$

If all 4 access Points covered:

$$P_4 = P_{c1} \times P_{c2} \times P_{c3} \times P_{c4}$$

Where P_{c1} , P_{c2} , P_{c3} , P_{c4} denote for the detection probabilities by each AP in the corner.

Based on this combined coverage probabilities, we can make the localization evaluation with CRLB more reasonable and practical. One fact we need to notice is that the coverage probabilities are only related with the fading margin $F\sigma$ and variance of shadow fading σ , which means if we change the value of σ , the result will be absolutely different.

5.2 CRLB with coverage probability and variable shadow fading

The Cramer-Rao Lower Bound (CRLB) sets a lower bound on the variance of any unbiased estimator. This can be extremely useful in several ways [46][47][48]:

1. If we find an estimator that achieves the CRLB, then we know that we have found an MVUE estimator.
2. The CRLB can provide a benchmark against which we can compare the performance of any unbiased estimator (We know we're doing very well if our estimator is "close" to the CRLB).
3. The CRLB enables us to rule-out impossible estimators. That is, we know that it is physically impossible to find an unbiased estimator that beats the CRLB. This is useful in feasibility studies.
4. The theory behind the CRLB can tell us if an estimator exists which achieves the bound.

In a word, Cramer Rao inequality provides lower bound for the estimation error variance. Minimum attainable variance is often larger than CRLB. We need to know the pdf to evaluate CRLB. Often we don't know this information and cannot evaluate this bound. If the data is multivariate Gaussian or i.i.d. with known distribution, we can evaluate it [49]. If the estimator reaches the CRLB, it is called efficient. Minimum-variance unbiased estimator (MVUE) may or may not be efficient. If it is not, we have to use other tools than CRLB to find it. It's not guaranteed that MVUE exists or is realizable [50][51].

In numerical, if we have an observation like $O = x + \eta$, which is a single observation in zero mean GN with variance σ^2 , we can see the probability density function as

$$f(O | \alpha) = \frac{1}{\sqrt{2\pi}\sigma} e^{-\frac{(O-x)^2}{2\sigma^2}}$$

Then we are able to compute the ML estimate:

$$\frac{\partial}{\partial x} \left\{ \ln \frac{1}{\sqrt{2\pi}\sigma} e^{-\frac{(O-x)^2}{2\sigma^2}} \right\} = 0 \Rightarrow -\frac{2(-1)(O_i - x)}{2\sigma_i^2} = 0 \Rightarrow \hat{x}_{ML} = E[x] = O$$

The variance of this estimate is the CRLB. In another word, the CRLB is the variance of the ML estimate and the inverse of the Fisher Matrix:

$$\begin{aligned} \mathbf{F} &= E \left[\frac{\partial \ln f(O/x)}{\partial x} \right]^2 = E \left[\frac{\partial}{\partial x} \left\{ \ln \frac{1}{\sqrt{2\pi}\sigma} - \frac{(O-x)^2}{2\sigma^2} \right\} \right]^2 \\ &= E \left[-\frac{2(-1)(O-x)}{2\sigma^2} \right]^2 = \frac{1}{\sigma^4} E[(O-x)^2]^2 = \frac{\sigma^2}{\sigma^4} = \frac{1}{\sigma^2} \Rightarrow CRLB = \mathbf{F}^{-1} = \sigma^2 \end{aligned}$$

Now we come to the RSS based localization problem, for RSS based localization we have:

$$P_r = P_0 - 10\alpha \log d + X(\sigma)$$

Gaussian noise is shadow fading. Based on this equation we can derive the common sense range estimate as:

$$\hat{d} = 10^{\frac{P_r - P_0}{10\alpha}}$$

So if we measure a feature of the signal, for example power, at a distance d , and we have an estimate distance \hat{d} . Then, the distance measurement error (DME) for ranging is $\varepsilon = d - \hat{d}$.

Here we want to observe \hat{d} so that we can find out the performance of localization. So we want to estimate distance based on the observation of power observation:

$$O = g(x) + \eta = P_r = P_0 - 10\alpha \log x + X(\sigma)$$

In this equation, $g(x) = P_0 - 10\alpha \log x$ and Gaussian noise is shadow fading.

Based on the probability density function we also have the ML estimate:

$$f(O/x) = \frac{1}{\sqrt{2\pi}\sigma} e^{-\frac{[O-g(x)]^2}{2\sigma^2}} \Rightarrow \hat{x}_{ML} = g^{-1}(O) = 10^{\frac{P_r - P_0}{10\alpha}}$$

Define a fisher matrix and calculate the variance of the ML estimate, we have:

$$\mathbf{F} = -E \left[\frac{\partial^2 \ln f(O/x)}{\partial x^2} \right] = E \left[\frac{\partial \ln f(O/x)}{\partial x} \right]^2 = \frac{[g'(x)]^2}{\sigma^2}$$

$$g'(x) = -\frac{10\alpha}{(\ln 10)x} \Rightarrow \mathbf{F} = \frac{(10)^2 \alpha^2}{(\ln 10)^2 \sigma^2 x^2}$$

Since the inverse of the variance of the ML estimate is the CRLB, the distance measurement error (CRLB) will be:

$$CRLB = \mathbf{F}^{-1} = \frac{(\ln 10)^2 \sigma^2}{100 \alpha^2} x^2 \Rightarrow \sigma_p \geq \frac{\ln 10 \sigma}{10 \alpha} x$$

This shows an interesting fact that the distance measurement error, the CRLB, is only related with the variance of the shadow fading σ and the distance x , which means as the shadow fading changes, CRLB will also be undoubtedly different.

Combined with the conclusion in section 5.1, we can reach a truth that not only the coverage probability but also CRLB are correlated with variance of shadow fading σ .

Upon this fact, we firstly use variable shadow fading instead of constant shadow fading (see in section 2.2) to calculate coverage probability and derive out the reliable distance, then among this distance we still use variable shadow fading to compute CRLB. In this way we can obtain the CRLB with coverage probability and variable shadow fading [52][53][54].

The revised CRLB with different number of APs are shown in figure 5.2:

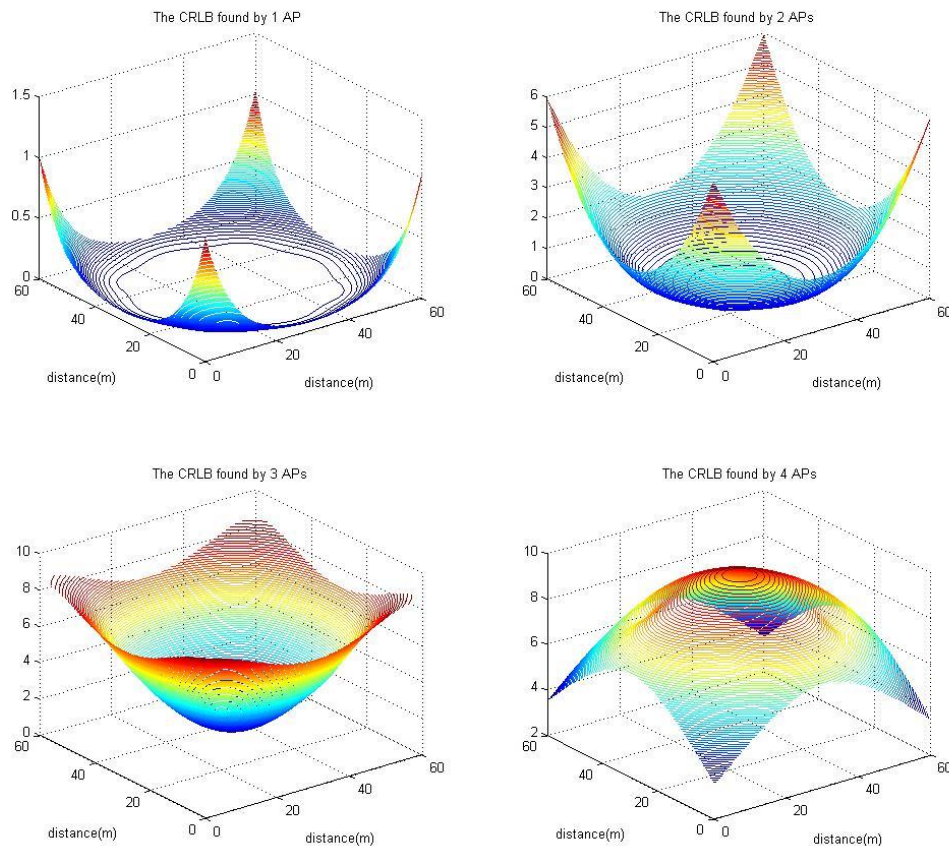


Figure 5.2 CRLB under practical conditions with different number of access points

We can also compute the overall CRLB under practical conditions which is shown in

figure 5.3:

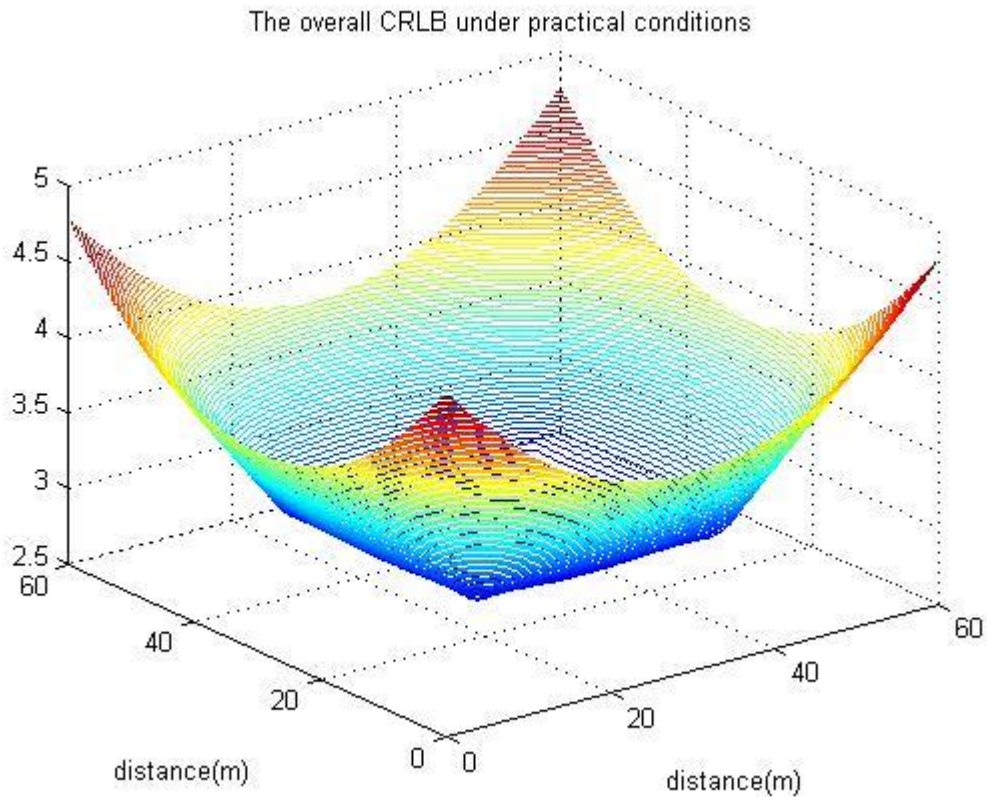


Figure 5.3 CRLB under practical conditions with all 4 access points

This is considered as the revised CRLB which takes into account both coverage probability and variable shadow fading. We can directly find that the performance shows best in the proximity near the APs (iBeacons), and the second best performance appears in the center area of the room, this is basically because this area is the most overlapped region which means the coverage probability is relatively higher than other regions that are not near the APs (iBeacons).

5.3 Discussions in CRLB with coverage probability and variable shadow fading

5.3.1 Comparison with traditional CRLB

In this section, we firstly define the localization scenario as 4 iBeacon deployed in the middle are of a room, which is considered as the most efficient deployment pattern according to the conclusion in section 4.3, shown in figure 5.4.

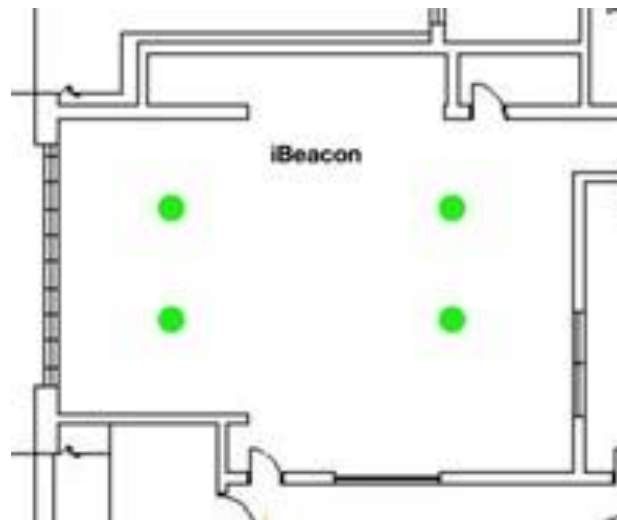


Figure 5.4 Scenario of localization using 4 iBeacons

In this scenario, if we calculate the CRLB under practical conditions, we will have such result shown in figure 5.5. And in order to compare with the traditional CRLB, we also provide the traditional result here in figure 5.6:

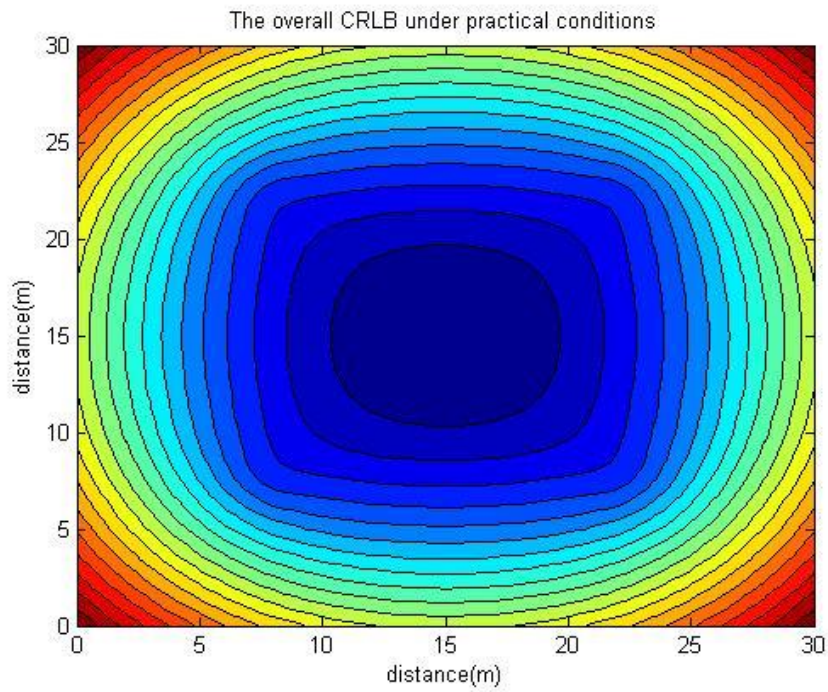


Figure 5.5 CRLB under practical conditions with 4 iBeacons

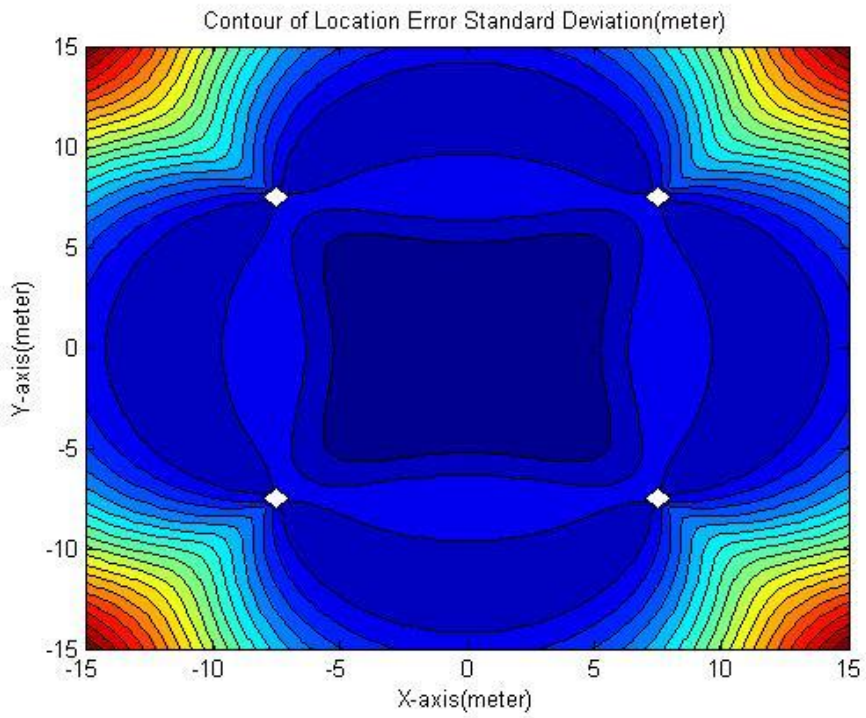


Figure 5.6 Traditional CRLB with 4 iBeacons

To show the comparison directly, both of the CDFs of CRLB in these two figures are calculated and we present the result in the figure 5.7 [55][56]:

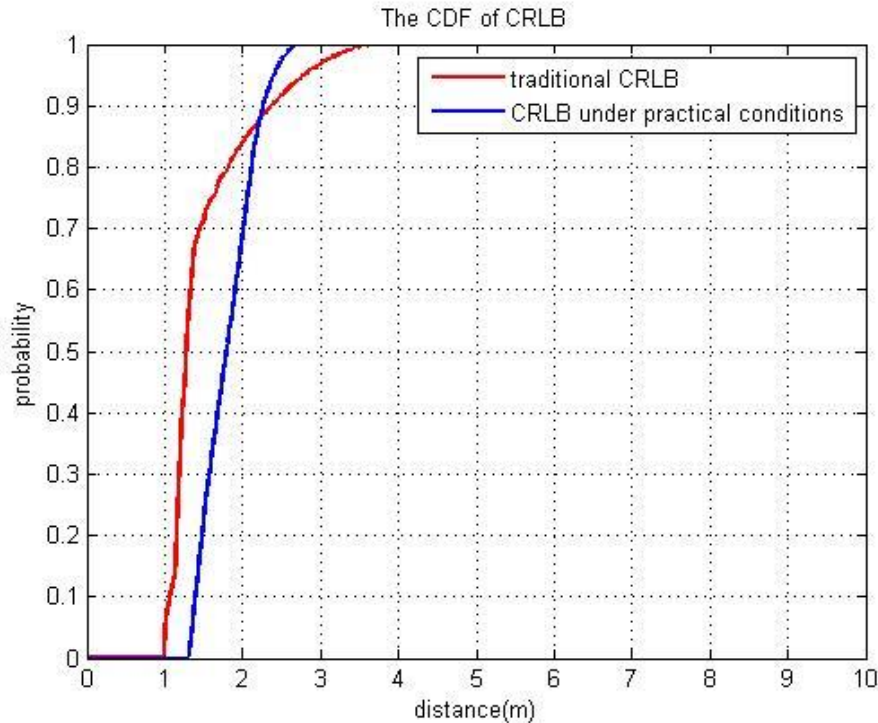


Figure 5.7 Comparison of cumulative distribution functions of traditional CRLB and CRLB under practical conditions

Obviously, the traditional CRLB seems better while the performance beyond 90% bound the CRLB under practical conditions performs better [57]. This is firstly because when we consider the fading margin, more power is needed to ensure the place can be discovered by iBeacon with a higher probability which we assume it is 100% in the traditional CRLB. Secondly, the introduction of variable variance of shadow fading makes the average variance of shadow fading much larger than the value we defined in the traditional CRLB that the variance of shadow fading is almost 4.28dB after 4m in the variable shadow fading while it is 2.5dB as we assumed in the tradition CRLB [13][58].

Besides, we compute and present the mean and standard variance of CDFs of two different CRLB in table 5.1:

	Mean of CDF	Standard variance of CDF
Traditional CRLB	1.5076m	0.5536m
Practical CRLB	1.8211m	0.3355m

Table 5.1 Mean and standard variance of cumulative distribution functions of traditional CRLB and CRLB under practical conditions

We can also obtain some similar conclusions in table 5.1 from figure 5.7 that the CDF of practical CRLB is almost on the right side of traditional CRLB which results in a larger mean. But the CDF of practical CRLB is closer (about 1m difference) than the traditional one (about 2.5m difference) which leads to a lower standard variance of CDF.

In conclusion, we can assert that the introduction of fading margin and variable shadow fading makes the CRLB higher but more stable. It is because larger average variance of shadow fading makes contributions to the higher CRLB, but the fading margin which leads to coverage probability makes the deviation of CRLB counteract with each other that equals to more stable CRLB.

5.3.2 Relationship between iBeacon coverage and room size

In order to describe the relationship between the CRLB and room size, we introduce a variable $\gamma = \frac{R}{D}$, where R is the reliable coverage defined by fading margin, D is the room size.

By now we have the overall CRLB considering coverage probability and variable shadow

fading, we calculate the mean and variance of that overall CRLB to see the tendency when γ increases. The results are shown in figure 5.8 and figure 5.9:

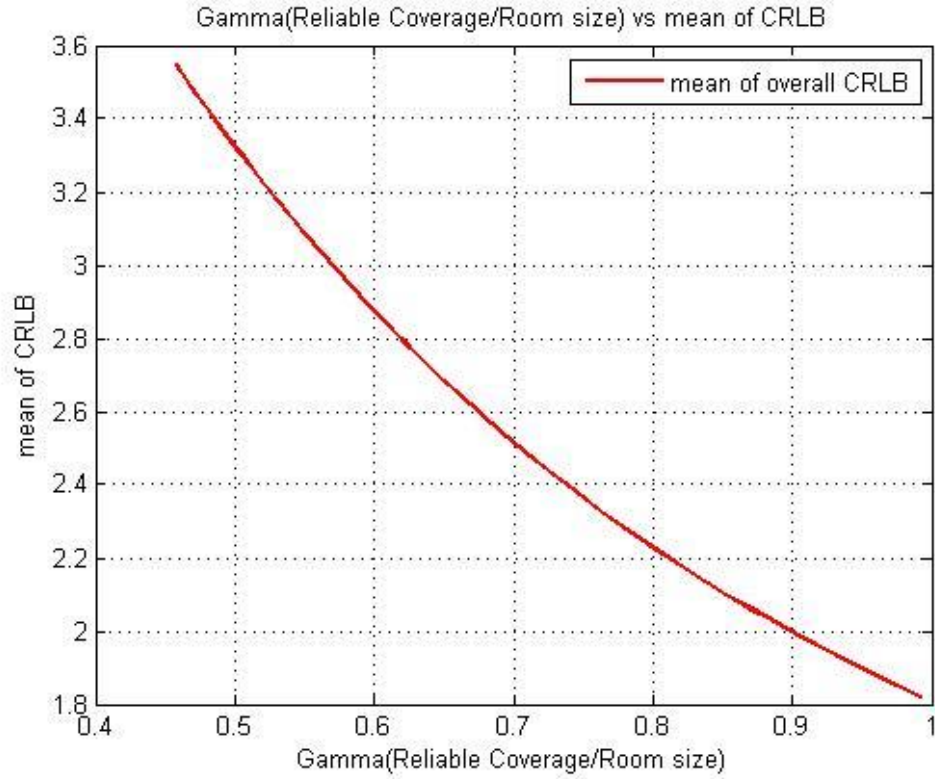


Figure 5.8 Mean of CRLB under practical conditions versus reliable coverage rate (reliable iBeacon coverage divided by room size)

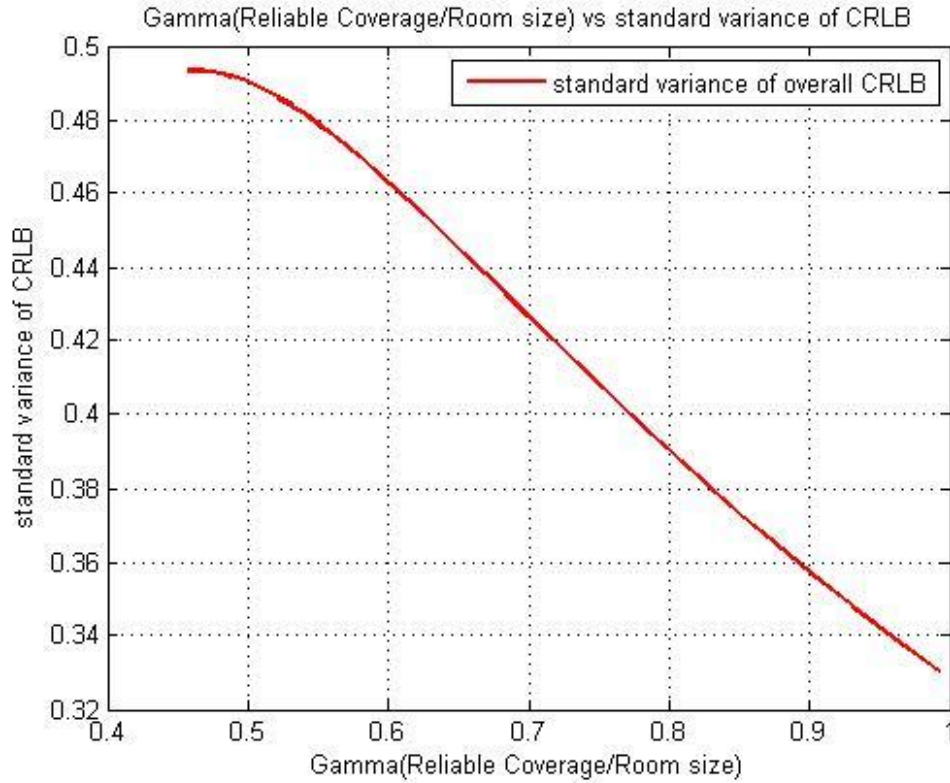


Figure 5.9 Standard variance of CRLB under practical conditions versus reliable coverage rate (reliable iBeacon coverage divided by room size)

Firstly we observe the variance of overall CRLB, the result seems reasonable [59][60]. As γ increases, which means the reliable coverage area becomes larger, the variance of overall CRLB is monotonically decreases. This conclusion is obvious because the variable shadow fading decreases with the room size becomes smaller (maximum distance becomes smaller), which in turn results in a lower CRLB, meanwhile, the reliable cover rate becomes larger that will decrease the variance of CRLB. When it comes to the mean of overall CRLB, we can also see the mean of overall CRLB monotonically decreases.

Apart from the mean and variance, we also calculate the cumulative distribution function

(CDF) of CRLB to show the whole performance versus γ . The result is shown in figure 5.10:

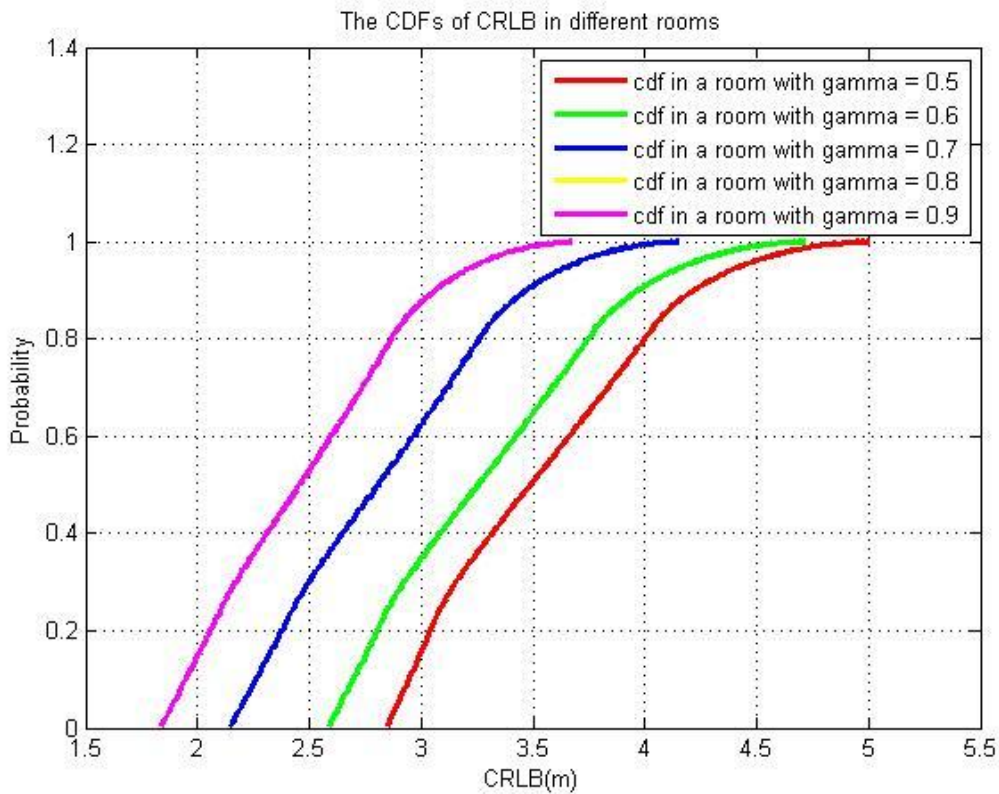


Figure 5.10 Comparison of cumulative distribution functions of CRLB under practical conditions in different reliable coverage rates

It is also a reasonable result that as γ increases, cdf of CRLB shifts left which denotes better performance. A typical conclusion we can make is that with smaller room size, CRLB becomes smaller and the localization accuracy becomes better. In a word, considering fading margin and variable shadow fading makes the calculation of CRLB more depend on the effective coverage rate γ , for $\gamma=R/D = 0.9$, we have a 90% bound in CDF of CRLB which is 3.17 meters with an improvement of 24.70% respect to $\gamma = 0.5$.

Chapter 6

Conclusions and future works

In chapter 1 and 2, we present the outlines and backgrounds of our project to obtain an overview of this thesis. Our motivation, contributions as well as some necessary information are introduced in these 2 chapters.

In chapter 3, we investigated and developed an iBeacon based intelligent in-room presence detection system to record the users in a room. We collected the RSSI data of iBeacon for LOS situation in a typical indoor office environment and we implement both single beacon and double beacons based approach. We also analyzed the probability density function, error detection rate and other metrics using the empirical measurement results. The optimal performance of our approach can be as high as 100%.

In chapter 4, we validated the probability to build a newborns localization and tracking system in hospitals by using iBeacon. In path-loss model part, we compare the CDF of DME of Estimote iBeacon model and our empirical path-loss model to demonstrate that using our model will have a better performance. More importantly, by simulations we directly observe the influence of different iBeacon deployment patterns and number of iBeacons in in-room localization, based on which we reasonably conclude that 5 iBeacons in the middle area performs best while 4 iBeacons in the middle is considered as the most efficient deployment pattern.

In chapter 5, we investigate the realistic relationship between localization accuracy and ratio of the iBeacon coverage and dimensions of the room using CRLB including influence on coverage probability and find out the dependence of variance of shadow fading on distance and effect on CRLB.

In summary, we firstly explain the main structures of the thesis, then we focus on the algorithms for intelligent in-room presence detection after the introduction about backgrounds. In addition to the presence detection system, we emphasize on the methodology for performance evaluation in in-room localization using iBeacon. We conclude the most efficient deployment pattern based on the analysis of CRLB. At last, practical conditions such as fading margin and variable shadow fading are taken into account in the calculation of CRLB and we also find out the relationship between the reliable iBeacon coverage and room size. In the future, we may testify the feasibility of using iBeacon for newborns localization in practice, and hopefully combine the accelerometer information [61][62] with localization to realize the tracking function for newborns in hospitals to make this whole project more practical and functional.

Bibliography

- [1] Kumar, P., Reddy, L., & Varma, S. (2009, December). Distance measurement and error estimation scheme for RSSI based localization in Wireless Sensor Networks. In *Wireless Communication and Sensor Networks (WCSN), 2009 Fifth IEEE Conference on* (pp. 1-4). IEEE.
- [2] Vaghefi, R. M., Gholami, M. R., & Ström, E. G. (2011, May). RSS-based sensor localization with unknown transmit power. In *Acoustics, Speech and Signal Processing (ICASSP), 2011 IEEE International Conference on* (pp. 2480-2483). IEEE.
- [3] Patwari, N., & Hero III, A. O. (2003, September). Using proximity and quantized RSS for sensor localization in wireless networks. In *Proceedings of the 2nd ACM international conference on Wireless sensor networks and applications* (pp. 20-29). ACM.
- [4] Binsabbar, M., & Zhang, N. (2014). An iphone application for providing ibeacon-based services to students.
- [5] Youn, S., Ahn, J. H., & Park, K. (2008, April). Entrance detection of a moving object using intensity average variation of subtraction images. In *Smart Manufacturing Application, 2008. ICSMA 2008. International Conference on* (pp. 459-464). IEEE.
- [6] Ivanov, B., Ruser, H., & Kellner, M. (2002, June). Presence detection and person identification in Smart Homes. In *Int. Conf. Sensors and Systems, St. Petersburg* (pp. 12-14).
- [7] Benezeth, Y., Laurent, H., Emile, B., & Rosenberger, C. (2011). Towards a sensor for detecting human presence and characterizing activity. *Energy and*

Buildings, 43(2), 305-314.

- [8] He, J., Geng, Y., Wan, Y., Li, S., & Pahlavan, K. (2013). A cyber physical test-bed for virtualization of RF access environment for body sensor network. *Sensors Journal, IEEE*, 13(10), 3826-3836.
- [9] Kohne, M., & Sieck, J. (2014, November). Location-based services with iBeacon technology. In *Artificial Intelligence, Modelling and Simulation (AIMS), 2014 2nd International Conference on* (pp. 315-321). IEEE.
- [10] What is iBeacon? A Guide to Beacons. <http://www.ibeacon.com/what-is-ibeacon-a-guide-to-beacons/>
- [11] Pahlavan, K., & Krishnamurthy, P. (2013). *Principles of wireless access and localization*. John Wiley & Sons.
- [12] Mailaender, L. (2011, September). Geolocation bounds for received signal strength (rss) in correlated shadow fading. In *Vehicular Technology Conference (VTC Fall), 2011 IEEE* (pp. 1-6). IEEE.
- [13] Liu, G. (2015). *Modeling and Performance Analysis of Hybrid Localization Using Inertial Sensor, RFID and Wi-Fi Signal* (Doctoral dissertation, Worcester Polytechnic Institute).
- [14] Martin, P., Ho, B. J., Grupen, N., Munoz, S., & Srivastava, M. (2014, November). An ibeacon primer for indoor localization: demo abstract. In *Proceedings of the 1st ACM Conference on Embedded Systems for Energy-Efficient Buildings* (pp. 190-191). ACM.
- [15] Geng, Y., Chen, J., Fu, R., Bao, G., & Pahlavan, K. (2015). Enlighten wearable physiological monitoring systems: On-body rf characteristics based human motion classification using a support vector machine.

- [16] Corna, A., Fontana, L., Nacci, A. A., & Sciuto, D. (2015, March). Occupancy detection via iBeacon on Android devices for smart building management. In *Proceedings of the 2015 Design, Automation & Test in Europe Conference & Exhibition* (pp. 629-632). EDA Consortium.
- [17] Bassbous, L., Guclu, G., & Steglich, S. (2014, October). Towards a remote launch mechanism of TV companion applications using iBeacon. In *Consumer Electronics (GCCE), 2014 IEEE 3rd Global Conference on* (pp. 538-539). IEEE.
- [18] Kim, C., & Lee, S. (2014, October). A research on Beacon code architecture extension using category and code Beacon structure. In *Information and Communication Technology Convergence (ICTC), 2014 International Conference on* (pp. 187-188). IEEE.
- [19] The manual of estimote iBeacons, <http://developer.estimote.com/>
- [20] Rodionov, D., Bushminkin, K., & Kolev, G. (2013, September). A Cooperative Localization Technique for Tracking in Hospitals and Nursing Homes. In *Healthcare Informatics (ICHI), 2013 IEEE International Conference on* (pp. 471-475). IEEE.
- [21] Cheng, S. H., Huang, J. C., & Lin, C. J. (2012, July). A real-time location and infant monitoring system based on active RFID. In *Machine Learning and Cybernetics (ICMLC), 2012 International Conference on* (Vol. 5, pp. 1844-1849). IEEE.
- [22] Ensworth, J. F., & Reynolds, M. S. (2015, April). Every smart phone is a backscatter reader: Modulated backscatter compatibility with bluetooth 4.0 low energy (ble) devices. In *RFID (RFID), 2015 IEEE International Conference on* (pp. 78-85). IEEE.
- [23] Yang, Y., Li, Z., & Pahlavan, K. Using iBeacon for Intelligent In-Room Presence Detection. *2016 IEEE International Multi-Disciplinary Conference on Cognitive Methods in Situation Awareness and Decision Support (CogSIMA), San Diego, CA,*

Mar. 2016.

- [24] Y. Yang Z. Li and K. Pahlavan. Using ibeacon for newborns localization in hospitals. *2016 IEEE 10th International Symposium on Medical Information and Communication Technology (ISMICT), Worcester, MA, Mar. 2016.*
- [25] Chen, Y., & Kobayashi, H. (2002). Signal strength based indoor geolocation. In *Communications, 2002. ICC 2002. IEEE International Conference on* (Vol. 1, pp. 436-439). IEEE.
- [26] Mailaender, L. (2011, March). On the CRLB scaling law for received signal strength (RSS) geolocation. In *Information Sciences and Systems (CISS), 2011 45th Annual Conference on* (pp. 1-6). IEEE.
- [27] Weiss, A. J. (2003). On the accuracy of a cellular location system based on RSS measurements. *Vehicular Technology, IEEE Transactions on*, 52(6), 1508-1518.
- [28] Gast, M. S. (2014). *Building applications with iBeacon: proximity and location services with bluetooth low energy*. " O'Reilly Media, Inc."
- [29] Newman, N. (2014). Apple ibeacon technology briefing. *Journal of Direct, Data and Digital Marketing Practice*, 15(3), 222-225.
- [30] Yang, J., & Chen, Y. (2009, November). Indoor localization using improved RSS-based lateration methods. In *Global Telecommunications Conference, 2009. GLOBECOM 2009. IEEE* (pp. 1-6). IEEE.
- [31] Pivato, P., Palopoli, L., & Petri, D. (2011). Accuracy of RSS-based centroid localization algorithms in an indoor environment. *Instrumentation and Measurement, IEEE Transactions on*, 60(10), 3451-3460.
- [32] Yang, J., Wang, Z., & Zhang, X. (2015). An ibeacon-based indoor positioning systems for hospitals. *International Journal of Smart Home*, 9(7), 161-168.

- [33] Leplawy, M. (2015). Indoors localization system with the use of WiFi and other network standards. *Przegląd Elektrotechniczny*, 91(1), 173-174.
- [34] Chen, Z., Zhu, Q., Jiang, H., & Soh, Y. C. (2015, June). Indoor localization using smartphone sensors and ibeacons. In *Industrial Electronics and Applications (ICIEA), 2015 IEEE 10th Conference on* (pp. 1723-1728). IEEE.
- [35] Gholami, M. R., Vaghefi, R. M., & Strom, E. G. (2013). RSS-based sensor localization in the presence of unknown channel parameters. *Signal Processing, IEEE Transactions on*, 61(15), 3752-3759.
- [36] Kim, S. C., Sung, Y. S., Kang, J. S., & Choi, J. (2007). Performance Evaluation of Positioning Techniques Based on UWB Radio.
- [37] Sand, S., Wang, W., & Dammann, A. (2012, September). Cramer-Rao lower bounds for hybrid distance estimation schemes. In *Vehicular Technology Conference (VTC Fall), 2012 IEEE* (pp. 1-5). IEEE.
- [38] Veletić, M., & Šunjevarić, M. (2014). On the Cramer-Rao lower bound for RSS-based positioning in wireless cellular networks. *AEU-International Journal of Electronics and Communications*, 68(8), 730-736.
- [39] Geng, Y., He, J., Deng, H., & Pahlavan, K. (2013, June). Modeling the effect of human body on TOA ranging for indoor human tracking with wrist mounted sensor. In *Wireless Personal Multimedia Communications (WPMC), 2013 16th International Symposium on* (pp. 1-6). IEEE.
- [40] Geng, Y., & Pahlavan, K. (2015). Design, Implementation and Fundamental Limits of Image and RF Based Wireless Capsule Endoscopy Hybrid Localization.
- [41] Geng, Y., Chen, J., & Pahlavan, K. (2013, September). Motion detection using RF signals for the first responder in emergency operations: A PHASER project.

- In *Personal Indoor and Mobile Radio Communications (PIMRC), 2013 IEEE 24th International Symposium on* (pp. 358-364). IEEE.
- [42] Geng, Y., He, J., & Pahlavan, K. (2013). Modeling the effect of human body on TOA based indoor human tracking. *International Journal of Wireless Information Networks*, 20(4), 306-317.
- [43] Geng, Y., He, J., & Pahlavan, K. (2013). Modeling the effect of human body on TOA based indoor human tracking. *International Journal of Wireless Information Networks*, 20(4), 306-317.
- [44] Yun, C. H., & So, J. (2015). A Bluetooth Beacon-Based Indoor Localization and Navigation System. *Advanced Science Letters*, 21(3), 372-375.
- [45] Tiwari, S., Wang, D., Fattouche, M., & Ghannouchi, F. (2012). A Hybrid RSS/TOA Method for 3D Positioning in an Indoor Environment. *ISRN Signal Processing*, 2012.
- [46] Prieto, J., Mazuelas, S., Bahillo, A., Fernández, P., Lorenzo, R. M., & Abril, E. J. Posterior Cramer-Rao Lower Bound for RSS/TOA-based Indoor Localization Systems.
- [47] Lieckfeldt, D., & Timmermann, D. Using Cramer-Rao-Lower-Bound to Reduce Complexity of Localization in Wireless Sensor Networks. In *BALTIC CONFERENCE* (p. 71).
- [48] Qaraqe, K. A., Hussain, S. I., Celebi, H., Abdallah, M., & Alouini, M. S. (2010, November). An RSS based location estimation technique for cognitive relay networks. In *Applied Sciences in Biomedical and Communication Technologies (ISABEL), 2010 3rd International Symposium on* (pp. 1-5). IEEE.
- [49] Shirahama, J., & Ohtsuki, T. (2008, May). RSS-based localization in environments with different path loss exponent for each link. In *Vehicular technology conference*,

2008. *VTC spring 2008. IEEE* (pp. 1509-1513). IEEE.
- [50] Stoyanova, T., Kerasiotis, F., Prayati, A., & Papadopoulos, G. (2007, October). Evaluation of impact factors on RSS accuracy for localization and tracking applications. In *Proceedings of the 5th ACM international workshop on Mobility management and wireless access* (pp. 9-16). ACM.
- [51] Kim, C. H., Hong, S. H., & Lee, S. W. (2015). A Research on Performance Improvement of iBeacon Using Transmission and Reception of Different Beacon Signals. *The Journal of Korean Institute of Communications and Information Sciences*, 40(1), 108-114.
- [52] Mailaender, L. (2012, June). Received Signal Strength (RSS) location estimation with nuisance parameters in correlated shadow fading. In *Communications (ICC), 2012 IEEE International Conference on* (pp. 3659-3663). IEEE.
- [53] Naik, U., & Bapat, V. N. (2013, October). Performance analysis of an indoor WLAN location estimation. In *Computational Intelligence and Information Technology, 2013. CIIT 2013. Third International Conference on* (pp. 524-526). IET.
- [54] Wang, Y., Ye, Q., Cheng, J., & Wang, L. (2015, December). RSSI-Based Bluetooth Indoor Localization. In *2015 11th International Conference on Mobile Ad-hoc and Sensor Networks (MSN)* (pp. 165-171). IEEE.
- [55] Vaghefi, R. M., & Buehrer, R. M. (2013, May). Received signal strength-based sensor localization in spatially correlated shadowing. In *ICASSP* (pp. 4076-4080).
- [56] Ciftler, B. S., Kadri, A., & Guvenc, I. (2015, March). Fundamental bounds on RSS-based wireless localization in passive UHF RFID systems. In *Wireless Communications and Networking Conference (WCNC), 2015 IEEE* (pp. 1356-1361). IEEE.

- [57] Denkovski, D., Angjelicinoski, M., Atanasovski, V., & Gavrilovska, L. (2012, October). Practical assessment of RSS-based localization in indoor environments. In *MILITARY COMMUNICATIONS CONFERENCE, 2012-MILCOM 2012* (pp. 1-6). IEEE.
- [58] Stojanović, D., & Stojanović, N. (2014). Indoor localization and tracking: Methods, technologies and research challenges. *Facta Universitatis, Series: Automatic Control and Robotics*, 13(1), 57-72.
- [59] Oksar, I. (2014, May). A Bluetooth signal strength based indoor localization method. In *Systems, Signals and Image Processing (IWSSIP), 2014 International Conference on* (pp. 251-254). IEEE.
- [60] Budina, J., Klapka, O., Kozel, T., & Zmitko, M. (2015). Method of iBeacon Optimal Distribution for Indoor Localization. In *Modeling and Using Context*(pp. 105-117). Springer International Publishing.
- [61] Palumbo, F., Barsocchi, P., Chessa, S., & Augusto, J. C. (2015, August). A stigmergic approach to indoor localization using Bluetooth Low Energy beacons. In *Advanced Video and Signal Based Surveillance (AVSS), 2015 12th IEEE International Conference on* (pp. 1-6). IEEE.
- [62] Xiao, B., Chen, H., & Zhou, S. (2007, June). A walking beacon-assisted localization in wireless sensor networks. In *Communications, 2007. ICC'07. IEEE International Conference on* (pp. 3070-3075). IEEE.

Appendix

A. Matlab code for path-loss modeling and Cramer-Rao

lower bound calculation:

```
clc;
close all;
clear all;

Pr0 = 52;
alpha = 2;
step = 0.5;
Xwall = 8:7:29;
x = 1:step:35.5;
num = length(x);
X = 10*log10(x);
WAF = unifrnd (0.3,0.7);
WAFdB = -10*log10(WAF);
noise = normrnd(0,2.5,1,num);
n = 1;
for r = 1:step:35.5;
    l(n) = floor((r-1)/7);
    Prr(n) = Pr0-10*alpha*log10(r)-l(n)*WAF;
    PrrCOM(n) = Pr0-10*alpha*log10(r);
    Pr(n) = Prr(n)+noise(n);
    PrCOM(n) = PrrCOM(n)+noise(n);
    p(n) = -10*log10(r);
    n = n+1;
end
pave = sum(p)/length(p);
Prave = sum(Pr)/length(Pr);
PrCOMave = sum(PrCOM)/length(PrCOM);
tempX1 = 0;
tempX2 = 0;
```

```

tempY = 0;
for i = 1:num;
    tempA1 = (p(i)-pave)*Pr(i);
    tempA2 = (p(i)-pave)*PrCOM(i);
    tempB = (p(i)-pave)^2;
    tempX1 = tempX1+tempA1;
    tempX2 = tempX2+tempA2;
    tempY = tempY+tempB;
end
alphaX1 = tempX1/tempY;
alphaX2 = tempX2/tempY;
Pr0X1 = Prave - alphaX1*pave;
Pr0X2 = PrCOMave - alphaX2*pave;
for j = 1:num
    PrX1(j) = Pr0X1-alphaX1*X(j);
    PrX2(j) = Pr0X2-alphaX2*X(j);
end
tempZ1 = 0;
tempZ2 = 0;
tempM1 = 0;
tempM2 = 0;
tempN1 = 0;
tempN2 = 0;
for ii = 1:num
    tempC1 = (PrX1(ii)-Prave)^2;
    tempC2 = (PrX2(ii)-PrCOMave)^2;
    tempD1 = (Pr(ii)-Prave)^2;
    tempD2 = (PrCOM(ii)-PrCOMave)^2;
    tempE1 = (Pr(ii)-PrX1(ii))^2;
    tempE2 = (PrCOM(ii)-PrX2(ii))^2;
    tempZ1 = tempZ1+tempC1;
    tempZ2 = tempZ2+tempC2;
    tempM1 = tempM1+tempD1;
    tempM2 = tempM2+tempD2;
    tempN1 = tempN1+tempE1;
    tempN2 = tempN2+tempE2;
end
R1 = tempZ1/tempM1;
R2 = tempZ2/tempM2;
SD1 = sqrt(tempN1/num);
SD2 = sqrt(tempN2/num);

```

```

P = Pr';
One = ones(num,1);
G = [One -X' -1'];
Beta = [Pr0 alpha WAF]';
BetaX = (G'*G)^(-1)*G'*P;
Pr0X3 = BetaX(1);
alphaX3 = BetaX(2);
PrX3 = G*BetaX;
Pave = sum(Pr)/num;
R3 = (BetaX'*G'*P-num*Pave^2)/(P'*P-num*Pave^2);
SD3 = sqrt(((P'-BetaX'*G')*P)/num);
plot(X,Pr,'r.',X,PrX1);
xlabel('10*log10 value of distance');
ylabel('RSS (dBm)');
title('Linear Regression');
grid on;
figure;
plot(X,Pr,'r.',X,PrX2);
xlabel('10*log10 value of distance');
ylabel('RSS (dBm)');
title('Compensated Linear Regression');
grid on;
figure;
plot(X,Pr,'r.',X,PrX3);
xlabel('10*log10 value of distance');
ylabel('RSS (dBm)');
title('Multiple Regression');
grid on;
figure;

```

```

%%%%%%%%%%%%%%%%%%%%%%%%%%%%%%%%%%%%%%%%%%%%%%%%%%%%%%%%%%%%%%%%%%%%%%%%

```

```

NUM = 5;
APx(1) = 15;
APy(1) = 15;
APx(2) = 15;
APy(2) = -15;
APx(3) = -15;
APy(3) = -15;
APx(4) = -15;

```

```

APy(4) = 15;
APx(5) = 0;
APy(5) = 0;
mx = -15:0.5:15;
my = -15:0.5:15;
nxy = length(mx);
SD0 = 2.5;
for yi = 1:nxy
    for xi = 1:nxy
        %if xi ~=
        for i1 = 1:NUM
            alpha2(i1) = 2.385;
            r(i1,xi,yi) = sqrt((mx(xi)-APx(i1))^2+(my(yi)-
APy(i1))^2);
            H1(i1,xi,yi) = -10*alpha2(i1)/(log(10))*(mx(xi)-
APx(i1))/r(i1,xi,yi)^2;
            H2(i1,xi,yi) = -10*alpha2(i1)/(log(10))*(my(yi)-
APy(i1))/r(i1,xi,yi)^2;
        end
        H(:, :, xi, yi) = [H1(:, xi, yi) H2(:, xi, yi)];
        Covv(:, :, xi, yi) = SD0^2*((H(:, :, xi, yi)'*H(:, :, xi, yi))^(-1));
        SDr(xi, yi) = sqrt(Covv(1,1,xi,yi)+Covv(2,2,xi,yi));
    end
end
SDr = SDr';
contourf(mx,my,SDr,20);
xlabel('X-axis(meter)');
ylabel('Y-axis(meter)');
title('Contour of Location Error Standard Deviation(meter)');
%%%%%%%%%%%%%%%%%%%%%%%%%%%%%%%%%%%%%%%%%%%%%%%%%%%%%%%%%%%%%%%%%%%%%%%%
SDrx = SDr;
SDrx(1,1) = 0;
SDrx(61,1) = 0;
SDrx(1,61) = 0;
SDrx(61,61) = 0;
SDrx(31,31) = 0;
step2 = 0.01;
range = 0:step2:10;
h = hist(SDrx,range);
cdf0 = cumsum(h)/(sum(h));
figure;

```

```

plot(range,cdf0,'r','linewidth',2);
grid on;
xlabel('Location Error Standard
Deviation(meter)'),ylabel('CDF'),title('The CDF of Location Error
Standard Deviation(meter)')

s = sum(SDrx);
meanx = sum(s)/(length(SDrx))^2;
variance = std(SDrx(:));

```

B. Matlab code for Cramer-Rao lower bound considering coverage probability and variable shadow fading:

```

clear all;close all;
%% basic path loss model
alpha1=2; % power gradient
lpmax=75; % max path loss in dB
%sigma1=8; % standard deviation of shadow fading
f=2.4e9; % transmitting frequency
c=3e8; % speed of light
lamda=c/f; % wave length
L0=40; % 1st meter path loss
pace=0.5;
reliability = 0.9;
%Distance=40;

t = 1;
o = 1;

for Distance = 30:1:65;
% x1=0;y1=0;
% x2=0;y2=Distance;
% x3=Distance;y3=Distance;
% x4=Distance;y4=0;
x1=Distance/4;y1=Distance/4;
x2=Distance/4;y2=3*Distance/4;
x3=3*Distance/4;y3=3*Distance/4;
x4=3*Distance/4;y4=Distance/4;

```

```

x=0:pace:Distance;y=0:pace:Distance;
L1=length(x);
r1=zeros(L1,L1);
r2=zeros(L1,L1);
r3=zeros(L1,L1);
r4=zeros(L1,L1);

for i=1:L1
    for j=1:L1
        r1(i,j)=sqrt((x(i)-x1)^2+(y(j)-y1)^2);
        r2(i,j)=sqrt((x(i)-x2)^2+(y(j)-y2)^2);
        r3(i,j)=sqrt((x(i)-x3)^2+(y(j)-y3)^2);
        r4(i,j)=sqrt((x(i)-x4)^2+(y(j)-y4)^2);
    end
end
lp1=L0+max(10*alpha1*log10(r1),-L0);
lp2=L0+max(10*alpha1*log10(r2),-L0);
lp3=L0+max(10*alpha1*log10(r3),-L0);
lp4=L0+max(10*alpha1*log10(r4),-L0);

alpha2=-4.28;
beta=0.9372;
gamma0=4.31;
sigma1=alpha2*exp(-beta*r1)+gamma0;
sigma2=alpha2*exp(-beta*r2)+gamma0;
sigma3=alpha2*exp(-beta*r3)+gamma0;
sigma4=alpha2*exp(-beta*r4)+gamma0;

for p=1:L1
    for q=1:L1
        pc1(p,q)=1-0.5*erfc((lpmax-lp1(p,q))/sqrt(2)/sigma1(p,q));
        pc2(p,q)=1-0.5*erfc((lpmax-lp2(p,q))/sqrt(2)/sigma2(p,q));
        pc3(p,q)=1-0.5*erfc((lpmax-lp3(p,q))/sqrt(2)/sigma3(p,q));
        pc4(p,q)=1-0.5*erfc((lpmax-lp4(p,q))/sqrt(2)/sigma4(p,q));
    end
end

[c1,h1] = contour(x,y,pc1','w','LevelList',[reliablity],'linewidth',3);
R1 = sqrt((c1(1,2)-x1)^2+(c1(2,2)-y1)^2);

if Distance == 60;

```

```

subplot(2,2,1);
[X1,Y1]=contourf(x,y,pc1',20);
xlabel('distance (m)'),ylabel('distance (m)'),title('The probabilities
found by AP1');
hold on;
[c1,h1] = contour(x,y,pc1', 'w', 'LevelList', [reliablity], 'linewidth', 3);
R1 = sqrt((c1(1,2)-x1)^2+(c1(2,2)-y1)^2);
clabel(c1,h1);

subplot(2,2,2);
[X2,Y2]=contourf(x,y,pc2',20);
xlabel('distance (m)'),ylabel('distance (m)'),title('The probabilities
found by AP2');
hold on;
[c2,h2] = contour(x,y,pc2', 'w', 'LevelList', [reliablity], 'linewidth', 3);
R2 = sqrt((c2(1,2)-x2)^2+(c2(2,2)-y2)^2);
clabel(c2,h2);

subplot(2,2,3);
[X3,Y3]=contourf(x,y,pc3',20);
xlabel('distance (m)'),ylabel('distance (m)'),title('The probabilities
found by AP3');
hold on;
[c3,h3] = contour(x,y,pc3', 'w', 'LevelList', [reliablity], 'linewidth', 3);
R3 = sqrt((c3(1,2)-x3)^2+(c3(2,2)-y3)^2);
clabel(c3,h3);

subplot(2,2,4);
[X4,Y4]=contourf(x,y,pc4',20);
xlabel('distance (m)'),ylabel('distance (m)'),title('The probabilities
found by AP4');
hold on;
[c4,h4] = contour(x,y,pc4', 'w', 'LevelList', [reliablity], 'linewidth', 3);
R4 = sqrt((c4(1,2)-x4)^2+(c4(2,2)-y4)^2);
clabel(c4,h4);
figure;
end

%% Coverage Probability
% 0 access is covered
p0=(1-pc1).* (1-pc2) .* (1-pc3) .* (1-pc4);

```

```

% 1 access point is covered
p11=pc1.*(1-pc2).*(1-pc3).*(1-pc4);
p12=pc2.*(1-pc1).*(1-pc3).*(1-pc4);
p13=pc3.*(1-pc1).*(1-pc2).*(1-pc4);
p14=pc4.*(1-pc1).*(1-pc2).*(1-pc3);
p1=p11+p12+p13+p14;
% 2 access points are covered
p21=pc1.*pc2.*(1-pc3).*(1-pc4);
p22=pc1.*pc3.*(1-pc2).*(1-pc4);
p23=pc1.*pc4.*(1-pc2).*(1-pc3);
p24=pc2.*pc3.*(1-pc1).*(1-pc4);
p25=pc2.*pc4.*(1-pc1).*(1-pc3);
p26=pc3.*pc4.*(1-pc1).*(1-pc2);
p2=p21+p22+p23+p24+p25+p26;
% 3 access points are covered
p31=pc1.*pc2.*pc3.*(1-pc4);
p32=pc1.*pc2.*pc4.*(1-pc3);
p33=pc1.*pc3.*pc4.*(1-pc2);
p34=pc2.*pc3.*pc4.*(1-pc1);
p3=p31+p32+p33+p34;
% 4 access points are covered
p4=pc1.*pc2.*pc3.*pc4;
pcheck=p1+p2+p3+p4;

%% Cramer Lower Bound

for m=1:1:L1
    for n=1:1:L1
        crlb1(m,n)=log(10)*r1(m,n)*sigma1(m,n)/(10*alpha1);
        crlb2(m,n)=log(10)*r2(m,n)*sigma2(m,n)/(10*alpha1);
        crlb3(m,n)=log(10)*r3(m,n)*sigma3(m,n)/(10*alpha1);
        crlb4(m,n)=log(10)*r4(m,n)*sigma4(m,n)/(10*alpha1);
    end
end

% 1 access point is covered
crlb11=crlb1;
crlb12=crlb2;
crlb13=crlb3;
crlb14=crlb4;
% 2 access points are covered

```

```

crlb21=(crlb1+crlb2)/2;
crlb22=(crlb1+crlb3)/2;
crlb23=(crlb1+crlb4)/2;
crlb24=(crlb2+crlb3)/2;
crlb25=(crlb2+crlb4)/2;
crlb26=(crlb3+crlb4)/2;
% 3 access points are covered
crlb31=(crlb1+crlb2+crlb3)/3;
crlb32=(crlb1+crlb2+crlb4)/3;
crlb33=(crlb1+crlb3+crlb4)/3;
crlb34=(crlb2+crlb3+crlb4)/3;
% 4 access points are covered
crlb41=(crlb1+crlb2+crlb3+crlb4)/4;

crlbt1=p11.*crlb11+p12.*crlb12+p13.*crlb13+p14.*crlb14;
crlbt2=p21.*crlb21+p22.*crlb22+p23.*crlb23+p24.*crlb24+p25.*crlb25+p26.*
crlb26;
crlbt3=p31.*crlb31+p32.*crlb32+p33.*crlb33+p34.*crlb34;
crlbt4=p4.*crlb41;
crlbt=(crlbt1+crlbt2+crlbt3+crlbt4)/4;

if Distance == 60;
subplot(2,2,1);
[C1,h1]=contour3(x,y,crlbt1,80);
xlabel('distance (m)'),ylabel('distance (m)'),title('The CRLB found by 1
AP');
subplot(2,2,2);
[C2,h2]=contour3(x,y,crlbt2,80);
xlabel('distance (m)'),ylabel('distance (m)'),title('The CRLB found by 2
APs');
subplot(2,2,3);
[C3,h3]=contour3(x,y,crlbt3,80);
xlabel('distance (m)'),ylabel('distance (m)'),title('The CRLB found by 3
APs');
subplot(2,2,4);
[C4,h4]=contour3(x,y,crlbt4,80);
xlabel('distance (m)'),ylabel('distance (m)'),title('The CRLB found by 4
APs');
figure;
CRLB60 = crlbt;
x60=0:pace:Distance;y60=0:pace:Distance;

```

```

end
%clabel(C,h);
crlb1mean(t) = mean(crlbt1(:),1);
crlb1std(t) = std(crlb1(:),0,1);
crlb2mean(t) = mean(crlbt2(:),1);
crlb2std(t) = std(crlb2(:),0,1);
crlb3mean(t) = mean(crlbt3(:),1);
crlb3std(t) = std(crlb3(:),0,1);
crlb4mean(t) = mean(crlbt4(:),1);
crlb4std(t) = std(crlb4(:),0,1);
crlbAllmean(t) = mean(crlbt(:),1);
crlbAllstd(t) = std(crlbt(:),0,1);

gamma2(t) = R1/Distance;
if gamma2(t) < 0.4
    CRLB1 = crlbt;
elseif gamma2(t) < 0.5
    CRLB2 = crlbt;
elseif gamma2(t) < 0.6
    CRLB3 = crlbt;
elseif gamma2(t) < 0.7
    CRLB4 = crlbt;
elseif gamma2(t) < 0.8
    CRLB5 = crlbt;
elseif gamma2(t) < 0.9
    CRLB6 = crlbt;
end
if t == 1
    gammamax = R1/Distance;
    CRLBend = crlbt;
    xmax=0:pace:Distance;ymax=0:pace:Distance;
end
t = t+1;
end

CRLBendmean(t) = mean(CRLBend(:));
CRLBendstd(t) = std(CRLBend(:));
[Cx,hx]=contourf(xmax,ymax,CRLBend,20);
xlabel('distance (m)'),ylabel('distance (m)'),title('The overall CRLB
under practical conditions');
figure;

```

```

[Cx,hx]=contour3(x60,y60,CRLB60,80);
xlabel('distance (m)'),ylabel('distance (m)'),title('The overall CRLB
under practical conditions');
step2 = 0.01;
range = 0:step2:10;
h = hist(CRLBend,range);
cdf3 = cumsum(h)/(sum(h));
load cdf4.mat
figure;
plot(range,cdf4,'r',range,cdf3,'linewidth',2);
legend('traditional CRLB','CRLB under practical conditions');
xlabel('distance (m)'),ylabel('probability'),title('The CDF of CRLB');
grid on;

figure;
plot(gamma2,crlbAllmean,'r','linewidth',2);
xlabel('Gamma (Reliable Coverage/Room size)');
ylabel('mean of CRLB');
title('Gamma (Reliable Coverage/Room size) vs mean of CRLB');
legend('mean of overall CRLB');
grid on;
figure;
plot(gamma2,crlbAllstd,'r','linewidth',2);
xlabel('Gamma (Reliable Coverage/Room size)');
ylabel('standard variance of CRLB');
title('Gamma (Reliable Coverage/Room size) vs standard variance of
CRLB');
legend('standard variance of overall CRLB');
grid on;

%% cdf
figure;
step = 0.01;
for k = 1:5
    if k == 1
        CRLB = CRLB2;
        Min = min(CRLB(:));
        Max = max(CRLB(:));
        range1 = Min:step:Max;
        h1 = hist(CRLB,range1);
        cdf1 = cumsum(h1)/(sum(h1));

```

```

elseif k == 2
    CRLB = CRLB3;
    Min = min(CRLB(:));
    Max = max(CRLB(:));
    range2 = Min:step:Max;
    h2 = hist(CRLB,range2);
    cdf2 = cumsum(h2)/(sum(h2));
elseif k == 3
    CRLB = CRLB4;
    Min = min(CRLB(:));
    Max = max(CRLB(:));
    range3 = Min:step:Max;
    h3 = hist(CRLB,range3);
    cdf3 = cumsum(h3)/(sum(h3));
elseif k == 4
    CRLB = CRLB5;
    Min = min(CRLB(:));
    Max = max(CRLB(:));
    range4 = Min:step:Max;
    h4 = hist(CRLB,range4);
    cdf4 = cumsum(h4)/(sum(h4));
elseif k == 5
    CRLB = CRLB5;
    Min = min(CRLB(:));
    Max = max(CRLB(:));
    range5 = Min:step:Max;
    h5 = hist(CRLB,range5);
    cdf5 = cumsum(h5)/(sum(h5));
end
end

plot(range1,cdf1,'r',range2,cdf2,'g',range3,cdf3,'bl',range4,cdf4,'y',ra
nge5,cdf5,'m','linewidth',2.5);
grid on;
xlabel('CRLB(m)'),ylabel('Probability'),title('The CDFs of CRLB in
different rooms');
legend('cdf in a room with gamma = 0.5','cdf in a room with gamma =
0.6','cdf in a room with gamma = 0.7','cdf in a room with gamma =
0.8','cdf in a room with gamma = 0.9');

```